

Published in final edited form as:

Eur J Radiol. 2014 January ; 83(1): 6–19. doi:10.1016/j.ejrad.2012.12.028.

A Practical Approach to High-Resolution CT of Diffuse Lung Disease

Mizuki Nishino, M.D.^{1,*}, Harumi Itoh, M.D., Ph.D.², and Hiroto Hatabu, M.D., Ph.D.^{3,*}

¹Department of Radiology, Dana-Farber Cancer Institute and Brigham and Women's Hospital, 450 Brookline Ave. Boston MA, 02215, USA, Mizuki_Nishino@DFCI.HARVARD.EDU, Phone: 617-582-7163 Fax: 617-582-8574

²Department of Radiology, University of Fukui Faculty of Medical Sciences, Matsuoka-cho, Yoshida-gun, Fukui, Japan. Phone: 81-776-61-8371

³Department of Radiology, Brigham and Women's Hospital, 75 Francis St., Boston, MA 02215, USA, Tel: 617-732-8353 Fax: 617-732-6336

Abstract

Diffuse lung disease presents a variety of high-resolution CT findings reflecting its complex pathology, and provides diagnostic challenge to radiologists. Frequent modification of detailed pathological classification makes it difficult to keep up with the latest understanding. In this review, we describe a practical approach to high-resolution CT diagnosis of diffuse lung disease, emphasizing 1) analysis of “distribution” of the abnormalities, 2) interpretation of “pattern” in relation to distribution, 3) utilization of associated imaging findings and clinical information, and 4) chronicity of the findings. This practical approach will help radiologists establish a way to interpret high-resolution CT, leading to pin-point diagnosis or narrower differential diagnoses of diffuse lung diseases.

Keywords

CT; high-resolution CT; diffuse lung disease; interstitial lung disease; lung

Introduction

Five years ago, an interventional radiologist in the Midwest made a request to one of the authors: “I read body CT cases once a week, which usually includes one or two cases of high-resolution CT of the lung. Will you give me a half-hour lesson so that I can dictate something more intelligent?” Throughout the following years, the author analyzed his own approach to high-resolution CT for diffuse lung diseases and discussed extensively with radiology colleagues and residents, which has resulted in this article to provide a practical

© 2013 Elsevier Ireland Ltd. All rights reserved.

All correspondence should be addressed to, Mizuki Nishino, M.D., Department of Radiology, Dana-Farber Cancer Institute and Brigham and Women's Hospital, 450 Brookline Ave. Boston MA, 02215, USA, Mizuki_Nishino@DFCI.HARVARD.EDU, Phone: 617-582-7163 Fax: 617-582-8574.

Publisher's Disclaimer: This is a PDF file of an unedited manuscript that has been accepted for publication. As a service to our customers we are providing this early version of the manuscript. The manuscript will undergo copyediting, typesetting, and review of the resulting proof before it is published in its final citable form. Please note that during the production process errors may be discovered which could affect the content, and all legal disclaimers that apply to the journal pertain.

Conflict of interest

Mizuki Nishino, Harumi Itoh, Hiroto Hatabu: None

approach to high-resolution CT of the diffuse lung disease for radiology residents and practicing radiologists. The authors believe that the interpretation of the distribution of the abnormalities, especially in relation to the secondary pulmonary lobule, gives important and direct clues for the differential diagnosis of high-resolution CT of diffuse lung diseases.

In this article, we provide a practical approach to diffuse lung diseases with emphasis on 1) analysis of “distribution” of the abnormalities, 2) interpretation of “pattern” in relation to distribution, 3) utilization of associated imaging findings and clinical information, and 4) chronicity of the findings. A flowchart is provided to summarize the approach (Fig. 1).

1. Diffuse Lung Disease: Present, or Not Present?

Before the interpretation of high-resolution CT images, it must be determined whether diffuse lung disease is present or not (Fig. 1). The common entity that must be differentiated from diffuse lung disease is dependent density/atelectasis. To differentiate diffuse lung disease from dependent density/atelectasis, additional images in the prone position may be useful (Fig. 2).

Once the presence of diffuse lung disease is established, the interpretation of high-resolution CT of diffuse lung diseases begins based on the following approaches: 1) analysis of “distribution” of the abnormalities, 2) interpretation of “pattern” in relation to distribution, 3) utilization of associated imaging findings and clinical information, and 4) chronicity of the findings.

2. Analyze “Distribution” of the Abnormalities

Analysis of the *distribution* of the abnormalities is the first and most important step in the interpretation of high-resolution CT of diffuse lung diseases (Fig. 1). The distribution is classified as follows: 1) upper, middle, lower lung distribution; 2) peripheral or central; and 3) distributions in relation to a secondary pulmonary lobule (i.e., lymphatic, centrilobular, and random).

2-1. Upper, middle and lower lung distribution, defined by dividing lungs into three areas in the cranio-caudal direction, helps to narrow the differential diagnoses for some diffuse lung disease have a predilection to involve upper lungs (i.e., sarcoidosis, hypersensitivity pneumonitis, silicosis), whereas other diffuse lung diseases tend to mainly involve lower lungs (i.e., idiopathic pulmonary fibrosis (IPF), non-specific interstitial pneumonia (NSIP)).

2-2. Peripheral or central distribution is also helpful for the same reason. Peripheral lung consists of two or three rows of secondary pulmonary lobules forming a layer of three to four centimeter in thickness at the lung periphery and along the lung surfaces adjacent to fissures, whereas the central lung consists of the remaining lung [1]. Some diseases characteristically favor peripheral distribution (i.e., cryptogenic organizing pneumonia, IPF), whereas other diseases such as cardiogenic pulmonary edema or alveolar proteinosis may manifest as central distribution. Some diseases with peripheral distribution such as IPF and NSIP tend to affect subpleural areas of the lung and extend along the pleura and fissures, which is sometimes described as “subpleural distribution”.

2-3. Secondary pulmonary lobule is a fundamental unit of lung structure and the key to understanding the distribution of diffuse lung disease [2]. Secondary pulmonary lobule represents a polygonal shaped structure composed of several acini conducted by terminal bronchiole. The number of acini in the secondary lobule is variable, ranging from 3 to over 20, depending upon the size of the lobule (Fig. 3A) [1–6]. The size of each secondary pulmonary lobule ranges between one and three cm. The interlobular septum defines the

boundary of the secondary pulmonary lobule. The bronchus and artery, or bronchovascular bundle, run into the center of the secondary pulmonary lobule (Fig. 3B) [1–6]. Analysis of which component of the secondary pulmonary lobule is involved is the key step to determine the distribution of the diffuse lung disease and narrow the differential diagnosis.

Lymphatic distribution

Pulmonary lymphatic system exists both along the bronchovascular bundle and interlobular septum. Therefore, diseases of the lymphatic system involve both the bronchovascular bundle and interlobular septa (Figs. 3B, 4) [1–6]. Note that the major and minor fissures are extensions of the pleura, and they belong to the same compartment. The major differential diagnoses of cases demonstrating lymphatic distribution are pulmonary edema, sarcoidosis, lymphangitic spread of tumor or lymphoma (Table 1).

Centrilobular distribution

Small airway related diseases present with predominantly bronchovascular bundle involvement, demonstrating centrilobular distribution (Fig. 5). The hallmark of the centrilobular distribution is the sparing of the interlobular septa unless the disease process completely fills the whole secondary pulmonary lobule.

Random distribution

When the distribution has no relation to secondary pulmonary lobule, it is called random distribution, which is often seen in miliary tuberculosis, hematogenous metastasis, and disseminated fungal infection.

It is important to perform preparatory analysis of the distribution, independent of the shape or morphologic pattern of the abnormalities. Once distribution has been determined, differential diagnosis of diffuse lung diseases on high-resolution CT can begin.

3. Could this be UIP or NSIP?

After determining the presence of a diffuse lung disease and analyzing the distribution, the next question to ask is: *“Could this be usual interstitial pneumonia (UIP) or nonspecific interstitial pneumonia (NSIP)?”* (Fig. 1). UIP and NSIP are the two most common forms of idiopathic interstitial lung disease. On high-resolution CT, UIP and NSIP show peripheral and basilar distribution often with decreased lung volumes. Honeycombing is common in UIP and is uncommon in NSIP. Clinical outcome and prognosis is substantially better in NSIP than in UIP [7, 8].

3-1. Usual interstitial pneumonia (UIP)

UIP is the histopathological abnormality with a hallmark of heterogeneous appearance at low magnification with alternating areas of normal lung, interstitial inflammation, fibrosis, and honeycomb change, with most severe involvement in the peripheral subpleural parenchyma [9]. Scattered clusters of fibroblasts and immature connective tissue within the pulmonary interstitium (so-called “fibroblastic focus”) is another key feature of UIP [8, 10].

The characteristic high-resolution CT features of UIP are: (1) peripheral and basilar distribution; (2) honeycombing; and (3) decreased lung volume unless associated with emphysema (Fig. 6). Traction bronchiectasis, interlobular septal thickening and ground glass opacities can also be present. It is important to pay particular attention to these key features of UIP, because of its poor prognosis.

Honeycombing is pathologically defined by the presence of small air-containing cystic spaces, generally lined by bronchiolar epithelium and having thickened walls composed of dense fibrous tissue, indicating the end-stage fibrotic lung disease [1]. On high-resolution CT, honeycombing is noted as clustered cystic air spaces (average size 0.3–1 cm) characterized by clearly definable 1–3 mm-thick walls, with predominantly peripheral and subpleural distribution (Fig. 6).

It should be noted that UIP is a histologic diagnosis and represents a lung reaction pattern to injury [1]. UIP can be idiopathic, in which case it is called idiopathic pulmonary fibrosis (IPF), or can be secondary to exposure to dusts (e.g., asbestos) or drugs (e.g., bleomycin), or can be associated with collagen vascular diseases [1]. Common differential diagnosis of diseases with histologic UIP pattern includes IPF, collagen vascular disease and asbestosis. Although these diseases share the main features on high-resolution CT, further differentiation may sometimes be possible based on the associated imaging findings, i.e., dilated esophagus in scleroderma or calcified pleural plaques in asbestosis, or based on the clinical information such as history of collagen vascular diseases or prior asbestos exposure (Fig. 7).

IPF is the clinical syndrome associated with the morphologic pattern of UIP [9]. Careful clinical evaluation to exclude an underlying etiology such as asbestos exposure or collagen vascular disease is necessary before making this diagnosis [1]. Clinically, IPF presents with progressive shortness of breath and nonproductive cough, which usually have been present for more than 6 months. The age at the time of presentation is usually over 50 years, and men are affected slightly more often than women. IPF does not usually respond to steroid treatment. The clinical course of IPF gradually deteriorates, sometimes with interspersed periods of more rapid decline [8, 9]. The prognosis of IPF is poor with median survival less than 5 years. Complications of IPF include accelerated progression, lung cancer and secondary infection [1, 11–13].

In a prospective study by Hunninghake et al, the positive predictive value of a confident diagnosis of UIP was 96% [14]. A confident diagnosis made on the basis of clinical and thin-section CT findings obviates the need for a lung biopsy. However, a confident CT diagnosis of UIP was not made in 25% – 50% of cases of histologically demonstrated UIP because of the lack of typical CT features, particularly honeycombing [8, 14].

3-2. Nonspecific interstitial pneumonia (NSIP)

NSIP, first described in 1994 by Katzenstein, is a histologic entity characterized by inflammation and fibrosis predominantly involving the alveolar walls [15]. Temporal and spatial homogeneity of this pattern is a key feature of NSIP, distinguishing it from UIP. The clinical symptoms of NSIP are similar to those of UIP, however, are usually milder. NSIP more commonly affects women and the mean age of presentation is usually about a decade younger than UIP [8, 10]. Importantly, NSIP has more favorable prognosis than that of UIP [1, 7, 8, 11, 12]. NSIP may be divided into cellular and fibrotic subtypes depending on the amounts of lung inflammation and fibrosis [8, 10]. Prognosis is poorer in patients with predominant fibrosis (fibrotic NSIP) than in those with inflammatory histologic findings (cellular NSIP) [16].

Characteristic high-resolution CT features of NSIP include basal-predominant ground glass opacities, traction bronchiectasis and lower lobe volume loss, with no or only mild honeycombing (Fig. 8) [8, 17–21]. However, there is considerable overlap in radiographic appearance between NSIP and UIP [17–21]. The CT features of cellular and fibrotic NSIP also overlap considerably [17]. Patients with predominant ground glass opacity are more

likely to respond to steroid treatment, and the parenchymal abnormalities of NSIP such as traction bronchiectasis and ground-glass opacity may be reversible at follow up [8, 17].

Histologic pattern of NSIP can be seen in an idiopathic manner or in relation to collagen vascular diseases, hypersensitivity pneumonitis, and drug-induced lung disease [8, 22]. Although associated imaging findings such as dilated esophagus in collagen vascular disease can be a clue of underlying disease (Fig. 9), differentiation between idiopathic NSIP and NSIP secondary to other causes is often difficult based on imaging findings alone, making clinical information necessary.

By recognizing the combination of characteristic high-resolution CT features, the most important and common category of UIP and NSIP can be ruled in or ruled out, which simplifies the following discussion of differential diagnoses of diffuse lung disease.

4. Interpretation of “Pattern” in relation to “Distribution”

Now, it is time to think about “pattern”. Note that even in the analysis of the patterns, it is important to keep the distribution of the patterns in mind, because the diseases presenting with the same morphological pattern but with different distributions have totally different differential diagnoses (Fig. 1). In this article, we introduce several useful patterns in relation to its distribution to help narrow the differential diagnosis.

In addition, when interpreting the patterns, the associated imaging findings (i.e., lymphadenopathy, pleural effusion) and the clinical information (i.e., symptoms such as hemoptysis and fever, heavy smoking history or prior exposure to certain substances), should be noted to reach a clinically relevant differential diagnosis. Chronicity of the findings, either suggested by the imaging features (i.e., architectural distortion indicating long-standing fibrotic changes or prior studies demonstrating chronic abnormalities) or by clinical history (i.e., acute/chronic onset, duration and progressiveness of the symptom), also help to further narrow the differential diagnosis.

4-1. Diseases of the lymphatic system

Diseases of the lymphatic system involve the interlobular septum, fissure and pleura, as well as bronchovascular bundles, and often demonstrate thickening of these structures. The interlobular septal thickening and bronchovascular bundle thickening can be smooth, irregular, or beaded, depending of the diseases. The major differential diagnoses are *pulmonary edema*, *sarcoidosis*, *lymphangitic spread of tumor or lymphoma* (Table 1).

Pulmonary edema is the most common entity among the diseases of the lymphatic system. It usually presents smooth interlobular septal thickening (Fig. 10). Associated imaging findings including diffuse ground glass opacities, pleural effusion, and cardiomegaly indicating congestive heart failure support this diagnosis. Clinical information about the presence/absence of congestive heart failure or other causes of pulmonary edema is also important. Because pulmonary edema is usually an acute process, the chronicity and the chronological changes of the findings should be examined by comparison with prior studies and by correlation with the clinical picture, such as onset of symptoms.

Sarcoidosis usually involves the lymphatic system with upper and middle lung distribution. Of note, sarcoidosis tends to demonstrate a beaded or irregular appearance with a thickened bronchovascular bundle, interlobular septum, fissure and pleura, reflecting its granulomatous nature (Fig. 11) [1, 11]. The associated imaging findings include symmetric and bilateral mediastinal and hilar lymphadenopathy, architectural distortion due to chronic inflammation, or extensive fibrosis in upper lung distribution with volume loss. The

associated clinical features including uveitis, elevated angiotensin-converting enzyme level, and sarcoidosis in other organ systems also help to support the diagnosis.

Lymphangitic spread of the tumor and lymphoma are diseases of the lymphatic system typically with lower lung distribution (Fig. 12). The involvement can be asymmetric. Associated imaging findings include lymphadenopathy in the mediastinum, axilla, supraclavicular areas and upper abdomen, which can be asymmetric or necrotic, and the presence of primary tumor or other metastasis in lymphangitic spread. In contrast to sarcoidosis, architectural distortion and extensive fibrosis are not usually present. The clinical information regarding underlying diseases is also important to consider.

4-2. Nodular lung disease

Random nodules—The hallmark of this useful pattern is random distribution of nodules in relation to the secondary pulmonary nodule. Nodular pattern can be further classified according to nodule size: (1) “*fine*” nodules (approximately 3 mm or less) and (2) “*medium or large*” sized nodules (> 3mm). Differential diagnosis for “fine” nodules with random distribution is *miliary tuberculosis, metastasis, and disseminated fungal infection* (Fig. 13). Major differential diagnosis for “medium or large” sized nodules with random distribution is *metastasis, metastasis, and metastasis*, however, tuberculosis and fungal infection can have fungal infections or tuberculosis can present with nodules that are larger than fine nodules especially in immunocompromised hosts (Fig. 14) (Table 1).

Centrilobular nodules—Centrilobular nodules are seen along the bronchovascular bundle (Fig 3B), indicating that the disease process is along the airway, most likely due to infection or inflammation. The nodules can be discrete or ill-defined (Fig. 15). On high-resolution CT images, it is critical to confirm absence of interlobular septal thickening in order to differentiate centrilobular nodules from diseases of lymphatic system. The etiology of the centrilobular nodules is usually benign, except for neoplasm spreading along the airway such as bronchoalveolar carcinoma or lymphoma, and includes a variety of diseases affecting centrilobular bronchioles [1] (Table 1). Diagnosis can be usually reached via bronchoscopy for most of the diseases demonstrating centrilobular nodules.

Centrilobular nodules are sometimes associated with branching opacities or “tree-in-bud” opacities, reflecting the presence of dilated centrilobular bronchioles impacted with mucus, fluid or pus [1]. These opacities also suggest airway-related infectious or inflammatory processes, including endobronchial spread of tuberculosis or atypical mycobacterial infection, infectious bronchiolitis and diffuse panbronchiolitis (Fig. 16) [1].

Nodules in lymphatic distribution—When nodules are in lymphatic distribution, the diseases of the lymphatic system, especially sarcoidosis, should be considered (Fig. 11) (Table 1). Lymphatic spread of the tumor or lymphoma may demonstrate nodules in lymphatic distribution. (Please see detailed discussion in Section 5.1).

4-3. Ground-glass opacity

Ground-glass opacity is defined as a non-specific term referring to “the presence on high-resolution CT of a hazy increase in lung opacity not associated with obscuration of underlying vessels” [1]. Ground-glass opacity implies a long list of differential diagnoses, almost anything occupying either alveoli or interstitium, or both. Therefore, in the interpretation of cases with ground-glass opacities, associated clinical information is often crucial. The differential diagnoses frequently encountered in the clinical setting are: hypersensitivity pneumonitis, diffuse infection such as *Pneumocystis jirovecii* pneumonia

(PCP) or cytomegalovirus (CMV) pneumonia, pulmonary edema and adult respiratory distress syndrome (ARDS), and diffuse pulmonary hemorrhage.

Analysis of distribution sometimes helps in differential diagnosis of ground-glass opacity. Central ground-glass opacity may indicate pulmonary edema if acute, or alveolar proteinosis if chronic. Peripheral ground-glass opacity can be seen in NSIP, COP and DIP. Centrilobular ground-glass opacity is often encountered in hypersensitivity pneumonitis and RB-ILD.

Hypersensitivity pneumonitis is an allergic lung disease that results from the inhalation of a variety of organic dust antigens, and is pathologically characterized by interstitial mononuclear cell infiltrate, cellular bronchiolitis and non-necrotizing epithelioid granulomas. Hypersensitivity pneumonitis is classified into three types; acute, subacute and chronic. There are limited reports about high-resolution CT findings in the acute phase, which occurs 4–8 hours from exposure. In the subacute phase, high-resolution CT demonstrates faint diffuse ground-glass opacity with somewhat centrilobular densities. Air trapping is almost always observed on expiratory high-resolution CT (Fig. 17). In the chronic phase, additional CT findings suggesting signs of scarring such as linear opacities and parenchymal distortion are seen, suggesting the chronicity of the disease. [1, 11]. Clinical information regarding exposure history to a certain antigen, as well as respiratory and constitutional symptoms is useful when interpreting high-resolution CT.

Diffuse infection including PCP and CMV pneumonia is an important differential diagnosis to be considered with ground-glass opacity, especially immunocompromised patients with infectious symptom (Fig. 18). Of note, PCP is a common cause of life-threatening opportunistic infection in patients with acquired immune deficiency syndrome (AIDS), and usually seen in patients with CD4 counts of less than 200 cells/mm³ [23].

Pulmonary edema is one of the most common diffuse lung diseases with groundglass opacity. High-resolution CT demonstrates ground-glass opacity in central distribution (Fig. 19), and is often associated with smooth interlobular septal thickening, as discussed previously. Causes of pulmonary edema vary, including both cardiogenic and noncardiogenic diseases.

ARDS is characterized by diffuse lung injury, leading to permeability edema and diffuse alveolar damage. High-resolution CT features include diffuse or patchy ground-glass opacity or consolidation, predominantly in dependent lung regions. The patients are often intubated because of severe respiratory distress. Clinically, ARDS is characterized by respiratory dyspnea and hypoxemia which develop over hours or days. The time course of the development and changes in the opacities should be carefully correlated with onset and changes in clinical symptoms.

Diffuse pulmonary hemorrhage demonstrates patchy or diffuse ground-glass opacity, and is sometimes accompanied by consolidation or ill-defined centrilobular opacities (Fig. 20). The causes of pulmonary hemorrhage are broad, including antglomerular basement membrane disease (Goodpasture's syndrome), vasculitis such as Wegener's granulomatosis and Churg-Strauss syndrome, collagen vascular diseases such as systemic lupus erythematosus, idiopathic pulmonary hemosiderosis, intrinsic or extrinsic coagulopathy, and drug reaction [11]. Specific diagnosis regarding the cause of hemorrhage is usually difficult on high-resolution CT findings, and clinical information about the underlying diseases is necessary for further differentiation among these diseases.

Pulmonary alveolar proteinosis is a disease characterized by filling of the alveolar spaces with a periodic acid-Schiff-positive lipid-rich proteinaceous material [1]. Pulmonary

alveolar proteinosis is most common in adults between 30 and 50 years old. Symptoms are usually mild and of insidious onset, and include nonproductive cough, fever, and mild dyspnea. High-resolution CT findings include bilateral ground-glass opacity in patchy or geographic distribution associated with smooth interlobular septal thickening (so-called crazy-paving) [1].

5. Advanced Problems

The basic approach described above will cover most of the diffuse lung disease cases encountered in daily clinical practice. However, there are still some disease categories that remain to be described. In this section, we will discuss advanced problems including smoking-related diffuse lung diseases, diffuse lung disease with increased lung volume, and bilateral multiple parenchymal opacities (Table 2).

5-1. Smoking-related diffuse lung diseases

Smoking-related diffuse lung diseases include respiratory bronchiolitis-associated interstitial lung Disease (RB-ILD), desquamative interstitial pneumonia (DIP), and Langerhans cell histiocytosis (LCH).

RB-ILD is a clinicopathologic entity characterized by symptomatic interstitial lung disease associated with pathologic lesions of respiratory bronchiolitis [1, 11, 12]. High-resolution CT features of RB-ILD include centrilobular ground-glass opacities, thickening of central and peripheral airways with associated centrilobular emphysema and air trapping. The disease predominantly affects the upper lobes [12, 24–26]. On histology, it demonstrates bronchiolocentric accumulation of pigmented alveolar macrophages with mild bronchiolar fibrosis and chronic inflammation.

DIP is a form of idiopathic interstitial pneumonia associated with cigarette smoking, and is characterized by the presence of increased numbers of pigmented macrophages evenly dispersed within alveolar spaces [13, 24–27]. High-resolution CT findings of DIP include ground-glass opacity with peripheral and patchy or diffuse distribution and uniform distribution with occasional interlobular septal thickening (Fig. 21). It has predominantly lower lung distribution [27]. Clinically, both RB-ILD and DIP affect cigarette smokers 30–40 years of age with a male-to-female ratio of 2:1. Pulmonary function tests demonstrate a restrictive abnormality and decreased DLCO. Significant overlap between RB-ILD and DIP is seen in clinical, radiological and pathological findings, and they are now considered to reflect different degrees of severity of the small airways and parenchymal reaction to cigarette smoking, with DIP being the end spectrum of RB-ILD [12, 24–26].

Pulmonary LCH is an uncommon diffuse lung disease histologically characterized by the destruction of distal airways by bronchocentric granulomas containing Langerhans cells [28–30]. The etiology is unknown; however, pulmonary LCH typically affects young adults and is associated with cigarette smoking [28–30]. High-resolution CT findings include a combination of cysts and nodules with centrilobular distribution and upper and middle lung predominance sparing the costophrenic angle (Fig.22). The cyst walls are commonly thin (hair-line) but can be as thick as several millimeters. The shape of the cysts is typically round but sometimes confluent or bizarre, and usually less than 1 cm in size; however, the cysts can be larger (2–3 cm) [1, 11]. Combinations of small nodules of varying sizes (1–5 mm, 5–10 mm, or larger) are seen, with indistinct margins. Cavitation of the nodule is often seen and is associated with a relatively thick wall [1, 11]. Lung volumes are normal or increased in most patients. Clinically, pulmonary LCH equally affects men and women, and is associated with smoking history. Prognosis varies from complete remission after smoking cessation to development of cystic lung disease.

5-2. Diffuse lung disease with increased lung volumes

Several diffuse lung diseases associated with increased lung volumes, including lymphangioleiomyomatosis (LAM), pulmonary LCH, and emphysema with fibrosis.

Lymphangioleiomyomatosis (LAM) is a rare, idiopathic disorder of the lung parenchyma characterized by diffuse interstitial proliferation of bundles of "immature" smooth muscle cells in the wall of enlarged air cavities [31]. High-resolution CT findings include multiple thin-walled cysts with diffuse and random distribution involving the costophrenic angles (Fig. 23). Cysts are clearly demarcated by thin even walls, and usually rounded shapes. Ground glass opacities or mild septal thickening may be seen. The lung volumes are increased. Associated imaging findings include recurrent pneumothorax and pleural effusion [1, 11, 32–34]. LAM affects almost exclusively females, characteristically at childbearing age. Symptoms include dyspnea on exertion, and sometimes with pneumothorax, leading to progressive loss of pulmonary function. Clinical course is usually slowly progressive, leading to respiratory failure and death. Treatment options include antiestrogen therapy and lung transplantation [1, 11, 32–34]. In contrast to LCH, LAM has no definite relation to smoking.

Differentiation between pulmonary LCH and LAM is often possible using clinicopathological and radiological features. The combination of cysts and nodules in pulmonary LCH helps to differentiate from LAM, which shows multiple thin-walled cysts with diffuse random distribution. The costophrenic angle involvement, which is not usually seen in pulmonary LCH but is present in LAM, is another clue.

Emphysema with fibrosis is relatively common and frequently encountered. Emphysema predominantly distributes centrally in upper and middle lung areas, whereas fibrosis predominantly distributes peripherally in lower lung area and base. In these cases, the combination of obstructive changes from emphysema and restrictive changes from fibrosis may demonstrate normal pulmonary function, which can be misleading. Awareness of this combination and evaluation on high-resolution CT is important.

5-3. Bilateral Multiple Parenchymal Opacities

Bilateral multiple parenchymal opacities are seen as multiple areas of increased lung attenuation, and are usually less round than nodules. Bilateral multiple parenchymal opacities include a long list of differential diagnoses, and possibly represent parenchymal processes of infection, neoplasm, or vasculitis or other inflammatory pathology. In the interpretation of bilateral multiple parenchymal opacities, the analysis of distribution is important: peripheral distribution of these opacities are often seen in organizing pneumonia (COP), chronic eosinophilic pneumonia (CEP), and thromboembolic diseases. At the same time, associated clinical information also plays a major role in this category with broad differential diagnosis.

In clinical practice, infection and neoplasm must be considered first. If they are not likely based on clinical correlations, categories such as interstitial lung disease and vasculitis should be considered next. Thromboembolic disease is a pitfall that should be kept in mind.

Infection—Bilateral multifocal parenchymal opacities can be seen in a variety of infectious processes, including bacterial or fungal infection. Among them, clinically important etiologies to be recognized include invasive aspergillosis, cryptococcosis, coccidioidomycosis, and nocardiasis. These organisms most typically affect immunocompromised patients. Invasive aspergillosis is characterized by involvement of normal lung tissue by *Aspergillus* organisms [1, 11]. High-resolution CT findings include

ill-defined nodular or consolidative opacities with surrounding ground glass opacities (halo sign) in early phase (Fig. 24), and cavitary nodules with air-crescent due to necrosis in late phase [1, 11]. Invasive aspergillosis is particularly common in neutropenic patients with immunosuppression.

Neoplasm—Some neoplastic processes can cause bilateral multifocal parenchymal opacities of the lung. The representative entities include bronchioalveolar cell carcinoma, lymphoma and lymphoproliferative disorders. Both bronchioalveolar cell carcinoma and lymphoma can present with bilateral multifocal parenchymal opacities, and differentiation between these two entities may be difficult on high-resolution CT (Fig. 25) [1, 11]. The appearance on high-resolution CT can be indistinguishable from that of pneumonia, and correlation with clinical symptoms and observation of chronicity and chronological changes of the finding by comparing prior studies are necessary.

Cryptogenic Organizing Pneumonia, Chronic Eosinophilic Pneumonia, and Vasculitis—Most cases of bilateral multiple parenchymal opacities presenting with fever and shortness of breath are thought to be caused by infectious processes and treated as such. However, in some cases, such treatment fails, making typical infectious process less likely. In these instances, atypical infection especially fungal infection as well as the next category of diseases, including cryptogenic organizing pneumonia (COP), chronic eosinophilic pneumonia (CEP) and vasculitis should be considered.

COP is characterized by the presence of granulation tissue within bronchiolar lumen and alveolar duct on histology [1, 11, 12]. COP, which was formerly called bronchiolitis obliterans organizing pneumonia (BOOP), refers to a disease with the histologic feature of organizing pneumonia of idiopathic cause [12]. On high-resolution CT, COP is characterized by patchy bilateral parenchymal consolidation with peripheral and lower lung distribution, and sometimes associated ground-glass opacities (Fig. 26) [1, 11, 12]. Histologic features of COP include buds of granulation tissue filling the bronchiolar lumen and alveolar ducts. Chronic inflammation and interstitial fibrosis of alveolar walls can be seen. The overall histologic feature has temporal homogeneity [1, 11, 12]. Clinical symptoms include cough, dyspnea, malaise, fever, and weight loss. Occasionally, COP resolves spontaneously, but often needs steroid treatment [1, 11, 12].

CEP is an idiopathic condition characterized by eosinophil-rich exudates in alveoli and interstitium on histology. On chest radiograph, the most classic findings are peripheral, non-segmental homogeneous consolidation with or without air-bronchogram, so-called “*photographic negative of pulmonary edema*” [11]. High-resolution CT features include patchy parenchymal consolidation with peripheral and upper lung distribution associated ground-glass opacities. Linear or band-like subpleural opacities may also be seen [1, 11]. Clinically, patients typically have a history of allergic diseases (atopic dermatitis, asthma, rhinitis, sinusitis, etc.). Symptoms include cough with mucoid sputum, high fever and night sweats that are severe and usually last more than 3 months. Peripheral eosinophilia is seen in 90% of patients [11].

As both COP and CEP are characterized by multiple consolidative opacities in peripheral distribution, the differentiation between the two entities can be difficult. Clinical information, especially peripheral eosinophilia, is important to further differentiate the entities.

Vasculitis includes a large and varied group of disorders characterized by inflammation and necrosis of blood vessels [11]. Frequency and manifestation of lung involvement in vasculitis vary greatly. Pulmonary vasculitides that typically present with bilateral

multifocal parenchymal opacities include Wegener's granulomatosis and allergic angiitis and granulomatosis (Churg-Strauss syndrome). However, they may also present with diffuse pulmonary hemorrhage, as seen in several other forms of pulmonary vasculitis.

Wegener's granulomatosis is characterized by necrotizing granulomatous vasculitis of the respiratory tract, segmental glomerulonephritis and small vessel vasculitis [1, 11]. Approximately 90% of patients have lung involvement. High-resolution CT findings include bilateral, multiple, rounded opacities with varying size in random distribution (Fig. 27). Cavitation is common, with a thick wall and irregular inner lining. Consolidation and ground glass opacities are often associated with pulmonary hemorrhage [1, 11]. Symptoms include sinusitis, cough, hemoptysis, or hematuria. More than 90% of patients have a positive serological test for cytoplasmic antineutrophil cytoplasmic antibody (cANCA), which is an important item of clinical information to support the diagnosis [1, 11].

Allergic angiitis and granulomatosis (Churg-Strauss syndrome) is characterized by necrotizing vasculitis, extravascular granuloma formation, and eosinophilic infiltration. It is a multisystem disorder with predilection for the lungs, skin, nervous system, gastrointestinal tract, heart, kidney and joints. High-resolution CT findings include air-space consolidation or ground glass opacities in a peripheral distribution, and multiple nodular lesions of varying size. Cavitation of nodules is less common compared to Wegener's granulomatosis [1, 11, 35]. Allergic diseases including asthma, nasal polyps and sinusitis are often present, and therefore, clinical history about these co-existent diseases should be examined.

Thromboembolic diseases—Thromboembolic disease is a pitfall of differential diagnosis in multiple parenchymal opacities. Although rare, patients with thromboembolism presenting with multiple parenchymal opacities on chest radiograph or CT can be misinterpreted to have any of the diffuse lung diseases described above. Therefore, it is important for radiologists to keep thromboembolic diseases in mind and to consider the possibility.

In pulmonary embolism with infarction, pleura-based or wedge-shaped opacities with increased attenuation and peripheral distribution are demonstrated on CT. These opacities do not show enhancement by intravenous contrast agent (if administered), representing pulmonary infarction [36]. **In pulmonary embolism without infarction**, multiple parenchymal opacities are also seen, commonly with lower lung distribution, representing atelectasis. When these findings are present, they should be correlated with clinical information including symptoms such as dyspnea, pleuritic chest pain, tachypnea, and tachycardia, D-dimer assay, and the presence/absence of deep venous thrombosis. When pulmonary embolism is suspected, pulmonary CT angiography should be performed to directly visualize emboli.

Septic embolism occurs when fragments of thrombus include micro-organisms, most typically bacteria [36]. On CT, septic embolism also demonstrates multiple parenchymal opacities, consisting of discrete nodules with varying degrees of cavitation and subpleural, wedge-shaped opacities, predominantly in the lower lobes (Fig. 28) [1, 36]. Common predisposing factors include tricuspid valve endocarditis with or without drug addiction, alcoholism, skin infection, and immunologic deficiencies (particularly lymphoma) [36, 37]. Infected venous catheters or pacemaker wires can also be a cause of septic embolism [1, 36].

6. Pitfall

The presence of underlying emphysema can modify the appearances of common conditions and make them look like unusual presentations of diffuse lung disease. Of particular

importance is emphysema with pneumonia, for this condition requires that the patient receive immediate treatment by antibiotics.

Conclusion

High-resolution CT of diffuse lung diseases provides broad differential diagnosis as well as diagnostic challenges. The practical approach described in this article focuses on the importance of distribution of the abnormalities and interpretation of pattern in relation to distribution. This approach is designed to provide a practical solution for radiologists who are facing the increasing necessity of interpreting high-resolution CT with advances in multidetector row CT technology.

Acknowledgments

The authors thank to radiology residents of Beth Israel Deaconess Medical Center and Brigham and Women's Hospital for constructive discussion. The gratitude is extended to Ms. Donna Wolfe, Mr. Michael Larson and Mr. Ronald Kukla for their assistance in manuscript preparation.

The investigators were supported by 1K23CA157631-01A1 (NCI) (M.N.), and 5R21 CA11627-02 (H.H.) from the National Institutes of Health

References

1. Webb, WR.; Muller, NL.; Naidich, DP. High-resolution CT of the lung. 3rd ed. Philadelphia, Pa: Lippincott Williams & Wilkins; 2000.
2. Webb WR. Thin-section CT of the secondary pulmonary lobule: anatomy and the image - the 2004 Fleischner lecture. *Radiology*. 2006; 239:322–338. [PubMed: 16543587]
3. Heitzman ER, Markarian B, Berger I, Dailey E. The secondary pulmonary lobule: a practical concept for interpretation of chest radiographs. II. Application of the anatomic concept to an understanding of roentgen pattern in disease states. *Radiology*. 1969; 93:513–519. [PubMed: 5822730]
4. Itoh H, Tokunaga S, Asamoto H, et al. Radiologic-pathologic correlations of small lung nodules with special reference to peribronchiolar nodules. *AJR*. 1978; 130:223–231. [PubMed: 414570]
5. Itoh H, Nakatsu M, Yoxtheimer LM, Uematsu H, Ohno Y, Hatabu H. Structural basis for pulmonary functional imaging. *Eur J Radiol*. 2001; 37:143–154. [PubMed: 11274842]
6. Itoh H, Nishino M, Hatabu H. Architecture of the lung: morphology and function. *J Thorac Imaging*. 2004; 19:221–227. [PubMed: 15502608]
7. Flaherty KR, Thwaite EL, Kazerooni EA, et al. Radiological versus histological diagnosis in UIP and NSIP: survival implications. *Thorax*. 2003; 58:143–148. [PubMed: 12554898]
8. Lynch DA, Travis WD, Müller NL, et al. Idiopathic interstitial pneumonias: CT features. *Radiology*. 2005; 236:10–21. Review. [PubMed: 15987960]
9. American Thoracic Society. Idiopathic pulmonary fibrosis: diagnosis and treatment—international consensus statement: American Thoracic Society (ATS), and the European Respiratory Society (ERS). *Am J Respir Crit Care Med*. 2000; 161:646–664. [PubMed: 10673212]
10. Mueller-Mang C, Grosse C, Schmid K, Stiebellehner L, Bankier AA. What Every Radiologist Should Know about Idiopathic Interstitial Pneumonias. *RadioGraphics*. 2007; 27:595–615. [PubMed: 17495281]
11. Wilson, AG.; Hansel, DM. Immunologic diseases of the lung. In: Armstrong, P.; Wilson, AG.; Dee, P.; Hansell, DM., editors. *Imaging of the diseases of the chest*. 3rd ed. London: Nw. Mosby; 2000. p. 533-636.
12. Wittram C, Mark EJ, McLoud TC. CT-histologic correlation of the ATS/ERS 2002 classification of idiopathic interstitial pneumonias. *Radiographics*. 2003; 23:1057–1071. [PubMed: 12975500]
13. Katzenstein AL, Myers JL. Idiopathic pulmonary fibrosis: clinical relevance of pathologic classification. *Am J Respir Crit Care Med*. 1998; 157:1301–1315. [PubMed: 9563754]

14. Hunninghake GW, Zimmerman MB, Schwartz DA, et al. Utility of a lung biopsy for the diagnosis of idiopathic pulmonary fibrosis. *Am J Respir Crit Care Med*. 2001; 164:193–196. [PubMed: 11463586]
15. Katzenstein AL, Fiorelli RF. Non-specific interstitial pneumonia/fibrosis: histologic patterns and clinical significance. *Am J Surg Pathol*. 1994; 18:136–147. [PubMed: 8291652]
16. Travis WD, Matsui K, Moss J, Ferrans VJ. Idiopathic nonspecific interstitial pneumonia: prognostic significance of cellular and fibrosing patterns—survival comparison with usual interstitial pneumonia and desquamative interstitial pneumonia. *Am J Surg Pathol*. 2000; 24:19–33. [PubMed: 10632484]
17. MacDonald SL, Rubens MB, Hansell DM, et al. Nonspecific interstitial pneumonia and usual interstitial pneumonia: comparative appearances at and diagnostic accuracy of thin-section CT. *Radiology*. 2001; 221:600–605. [PubMed: 11719652]
18. Hartman TE, Swensen SJ, Hansell DM, et al. Nonspecific interstitial pneumonia: variable appearance at high-resolution chest CT. *Radiology*. 2000; 217:701–705. [PubMed: 11110931]
19. Screaton NJ, Hiorns MP, Lee KS, et al. Serial high resolution CT in non-specific interstitial pneumonia: prognostic value of the initial pattern. *Clin Radiol*. 2005; 60:96–104. [PubMed: 15642299]
20. Kim TS, Lee KS, Chung MP, et al. Nonspecific interstitial pneumonia with fibrosis: high-resolution CT and pathologic findings. *AJR Am J Roentgenol*. 1998; 171:1645–1650. [PubMed: 9843306]
21. Elliot TL, Lynch DA, Newell JD Jr, et al. High-resolution computed tomography features of nonspecific interstitial pneumonia and usual interstitial pneumonia. *J Comput Assist Tomogr*. 2005; 29:339–345. [PubMed: 15891504]
22. Desai SR, Veeraraghavan S, Hansell DM, et al. CT features of lung disease in patients with systemic sclerosis: comparison with idiopathic pulmonary fibrosis and nonspecific interstitial pneumonia. *Radiology*. 2004; 232:560–567. [PubMed: 15286324]
23. Armstrong, P.; Dee, P. AIDS and other forms of immunocompromise. In: Armstrong, P.; Wilson, AG.; Dee, P.; Hansell, DM., editors. *Imaging of the diseases of the chest*. 3rd ed. London: Nw. Mosby; 2000. p. 255–303.
24. Ryu JH, Myers JL, Swensen SJ. Bronchiolar disorders. *Am J Respir Crit Care Med*. 2003; 168:1277–1292. [PubMed: 14644923]
25. Moon J, du Bois RM, Colby TV, Hansell DM, Nicholson AG. Clinical significance of respiratory bronchiolitis on open lung biopsy and its relationship to smoking related interstitial lung disease. *Thorax*. 1999; 54:1009–1014. [PubMed: 10525560]
26. Heyneman LE, Ward S, Lynch DA, et al. Respiratory bronchiolitis, respiratory bronchiolitis-associated interstitial lung disease, and desquamative interstitial pneumonia: different entities or part of the spectrum of the same disease process? *AJR*. 1999; 173:1617–1622. [PubMed: 10584810]
27. Hartman TE, Primack SL, Swensen SJ, et al. Desquamative interstitial pneumonia: thin-section CT findings in 22 patients. *Radiology*. 1993; 187:787–790. [PubMed: 8497631]
28. Abbott GF, Rosado-de-Christenson ML, Franks TJ, Frazier AA, Galvin JR. From the archives of the AFIP: pulmonary Langerhans cell histiocytosis. *Radiographics*. 2004; 24:821–841. [PubMed: 15143231]
29. Travis WD, Borok Z, Roum JH, et al. Pulmonary Langerhans cell granulomatosis (histiocytosis X): a clinicopathologic study of 48 cases. *Am J Surg Pathol*. 1993; 17:971–986. [PubMed: 8372949]
30. Vassallo R, Jensen EA, Colby TV, et al. The overlap between respiratory bronchiolitis and desquamative interstitial pneumonia in pulmonary Langerhans cell histiocytosis: high-resolution CT, histologic, and functional correlations. *Chest*. 2003; 124:1199–1205. [PubMed: 14555547]
31. Pallisa E, Sanz P, Roman A, Majo J, Andreu J, Caceres J. Lymphangioleiomyomatosis: pulmonary and abdominal findings with pathologic correlation. *Radiographics*. 2002; 22:S185–S198. [PubMed: 12376610]
32. Kalassian KG, Doyle R, Kao P, Ruoss S, Raffin TA. Lymphangioleiomyomatosis: new insights. *Am J Respir Crit Care Med*. 1997; 155:1183–1186. [PubMed: 9105053]

33. Taylor JR, Ryu J, Colby TV, Raffin TA. Lymphangioleiomyomatosis: clinical course in 32 patients. *N Engl J Med.* 1990; 323:1254–1260. [PubMed: 2215609]
34. Sullivan EJ. Lymphangioleiomyomatosis: a review. *Chest.* 1998; 114:1689–1703. [PubMed: 9872207]
35. Seo JB, Im JG, Chung JW. Pulmonary vasculitis: the spectrum of radiological findings. *Br J Radiol.* 2000; 73:1224–1231. [PubMed: 11144805]
36. Han D, Lee KS, Franquet T, et al. Thrombotic and nonthrombotic pulmonary arterial embolism: spectrum of imaging findings. *Radiographics.* 2003; 23:1521–1539. [PubMed: 14615562]
37. Roberts WC, Buchbinder NA. Right-sided valvular infective endocarditis: a clinicopathologic study of twelve necropsy patients. *Am J Med.* 1972; 53:7–19. [PubMed: 4402567]

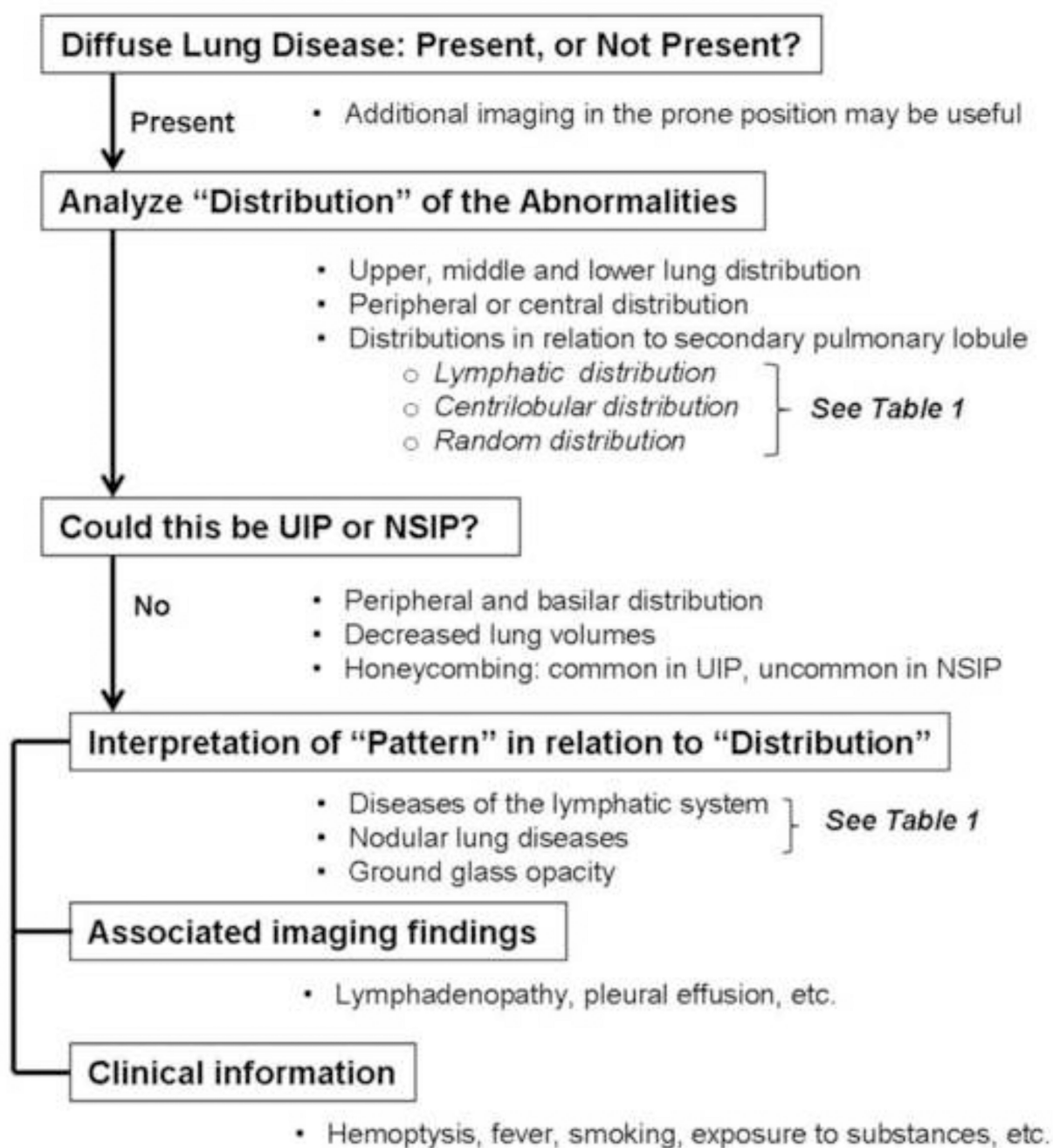
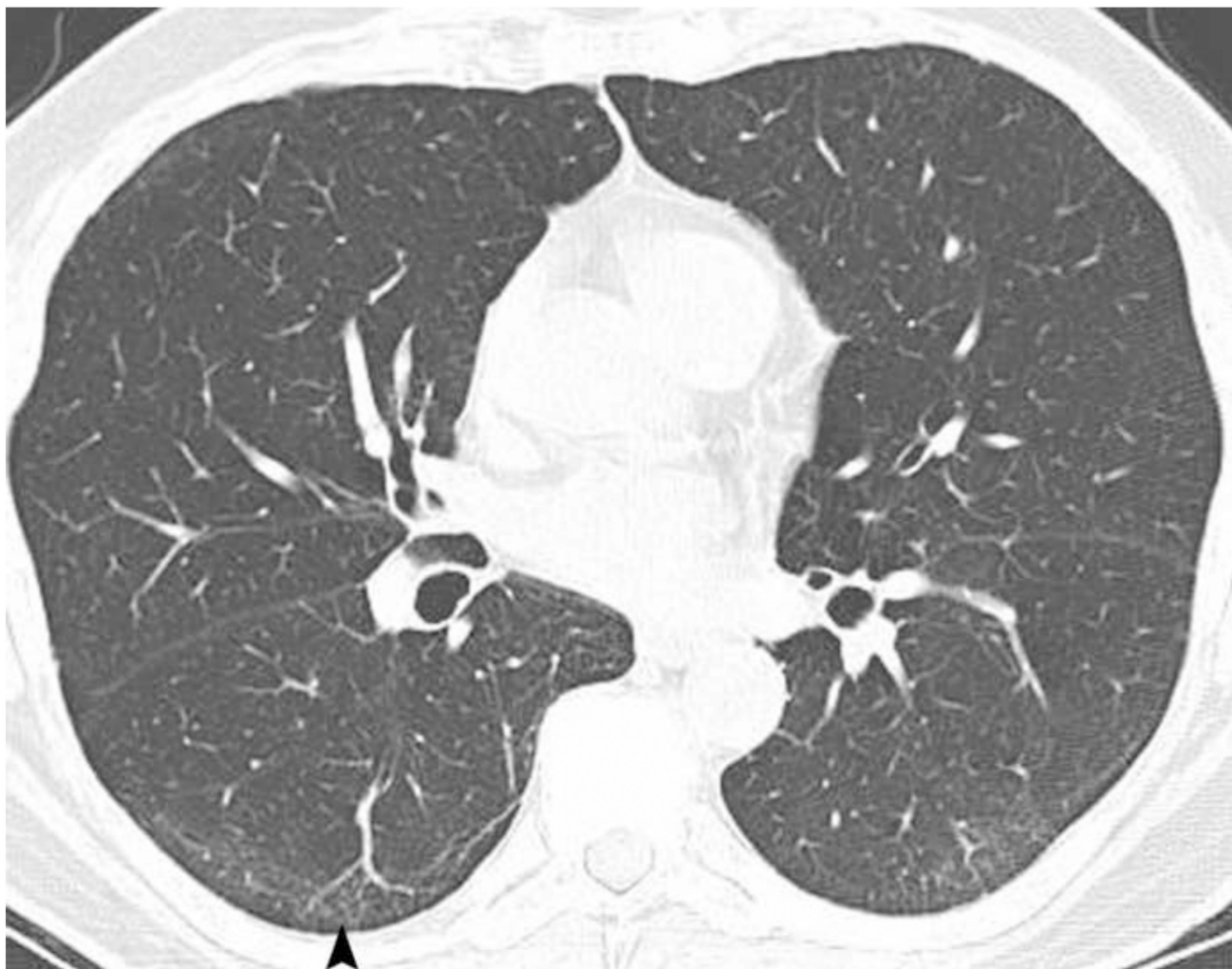


Figure 1. A flowchart summarizing a practical approach to HRCT of diffuse lung disease

A



B

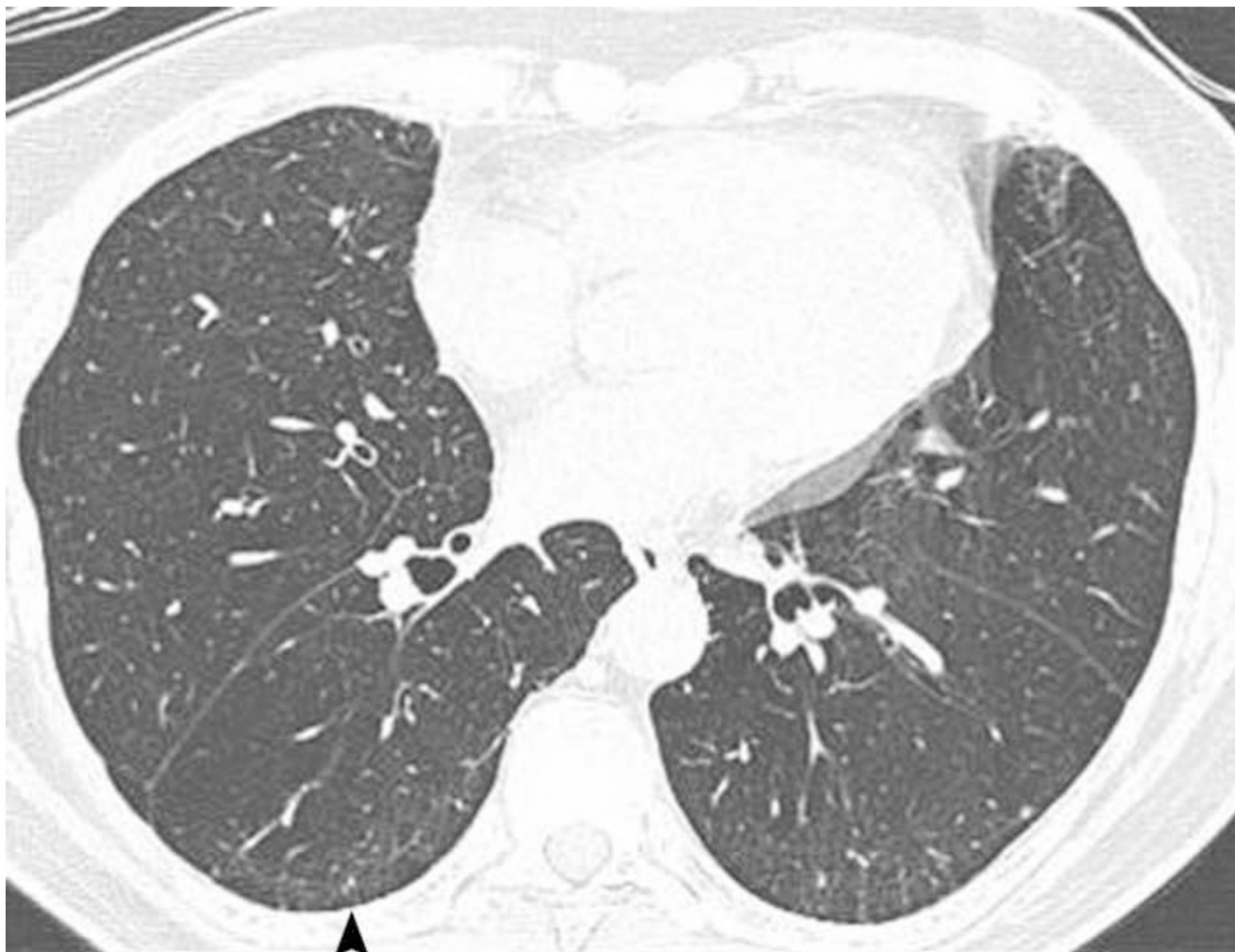
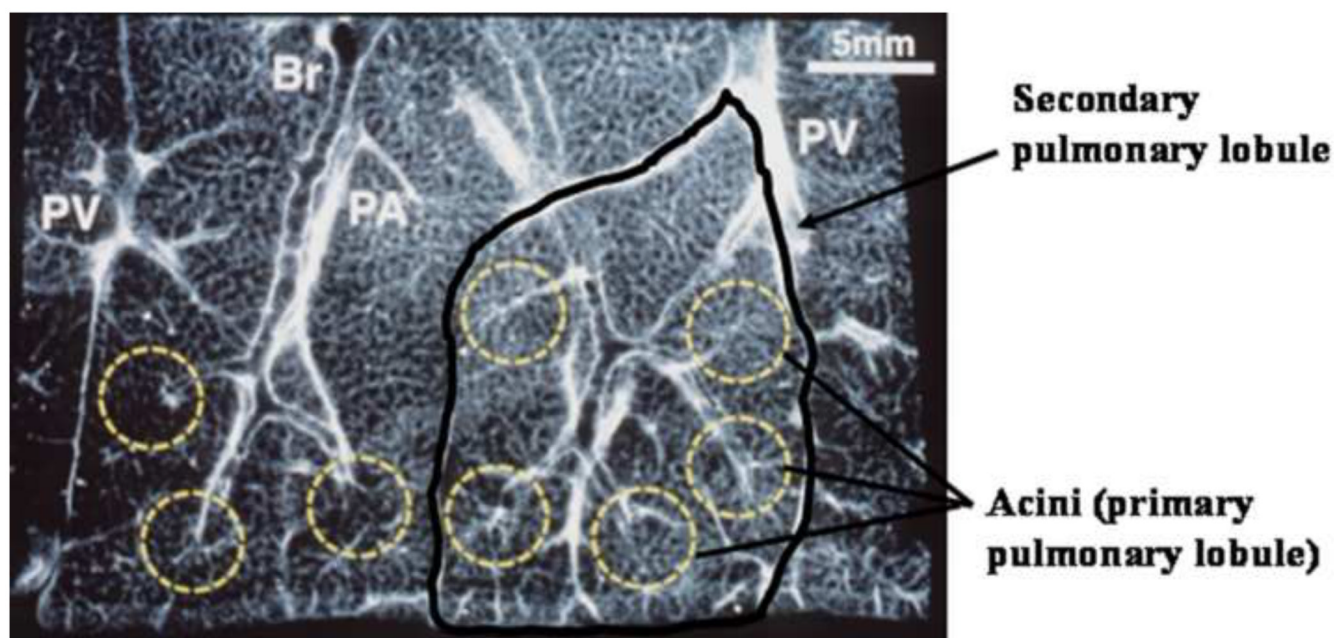


Figure 2. Diffuse lung disease: present or not present

A. Supine high-resolution CT image of the lung shows faint opacities in the dependent portion of the lung, requiring differentiation between diffuse lung disease versus dependent opacities.

B. On a prone high-resolution CT image at a similar level, the dependent opacities persist, indicating that the opacities are not gravity-dependent, and confirms the presence of diffuse lung disease.

A

B**Figure 3. Secondary pulmonary lobule**

A. Radiograph of 1-mm thick section of lung specimen demonstrates a polygonal structure composed of several acini conducted by terminal bronchioles, representing a secondary pulmonary lobule.

B. Radiograph of 1-mm thick section of lung specimen shows interlobular septum (arrowheads) which defines the boundary of the secondary pulmonary lobule and the bronchovascular bundles (arrows), which run into the center of the secondary pulmonary lobule.

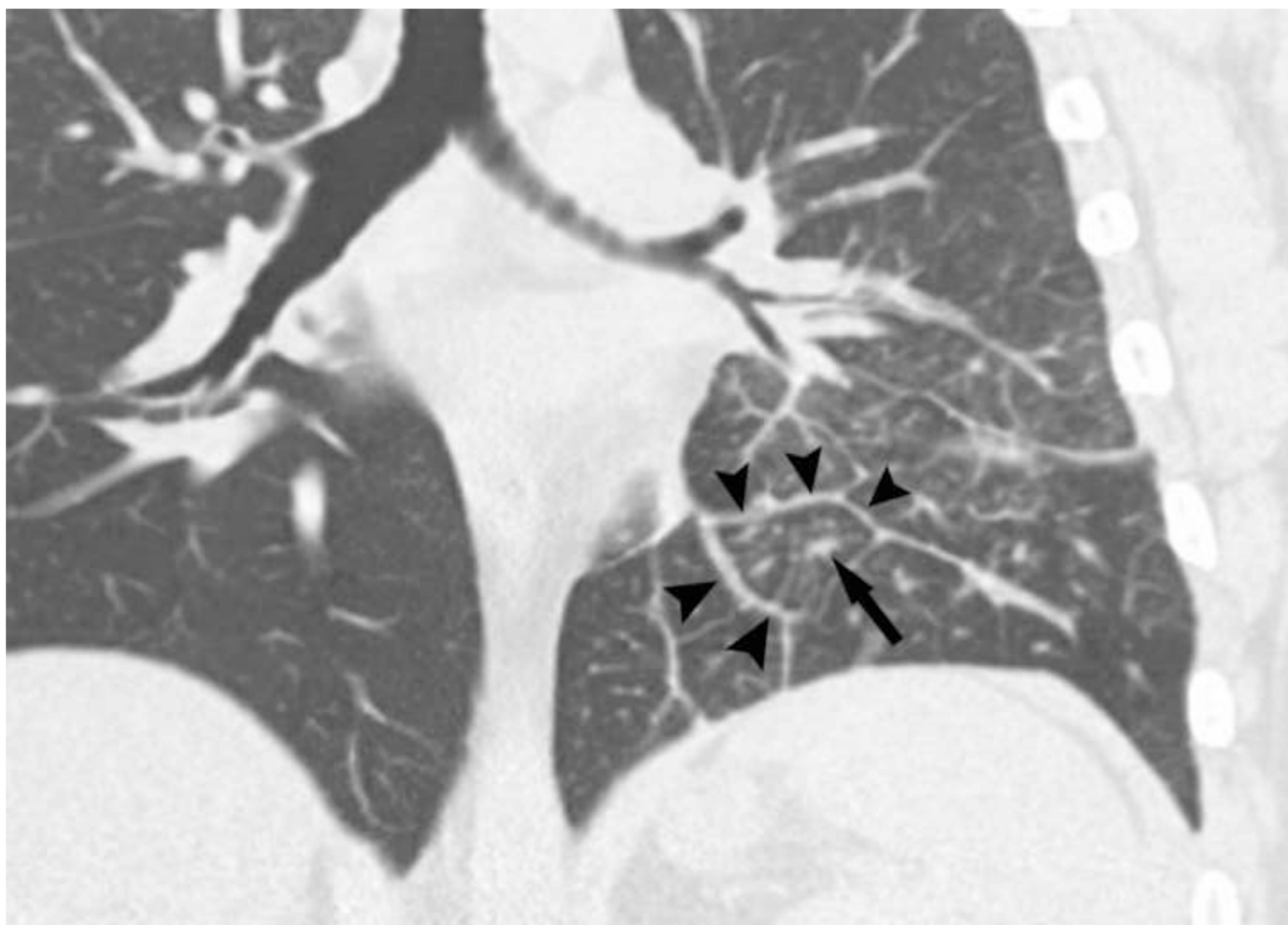


Figure 4. Lymphatic distribution: Lymphangitic spread of tumor

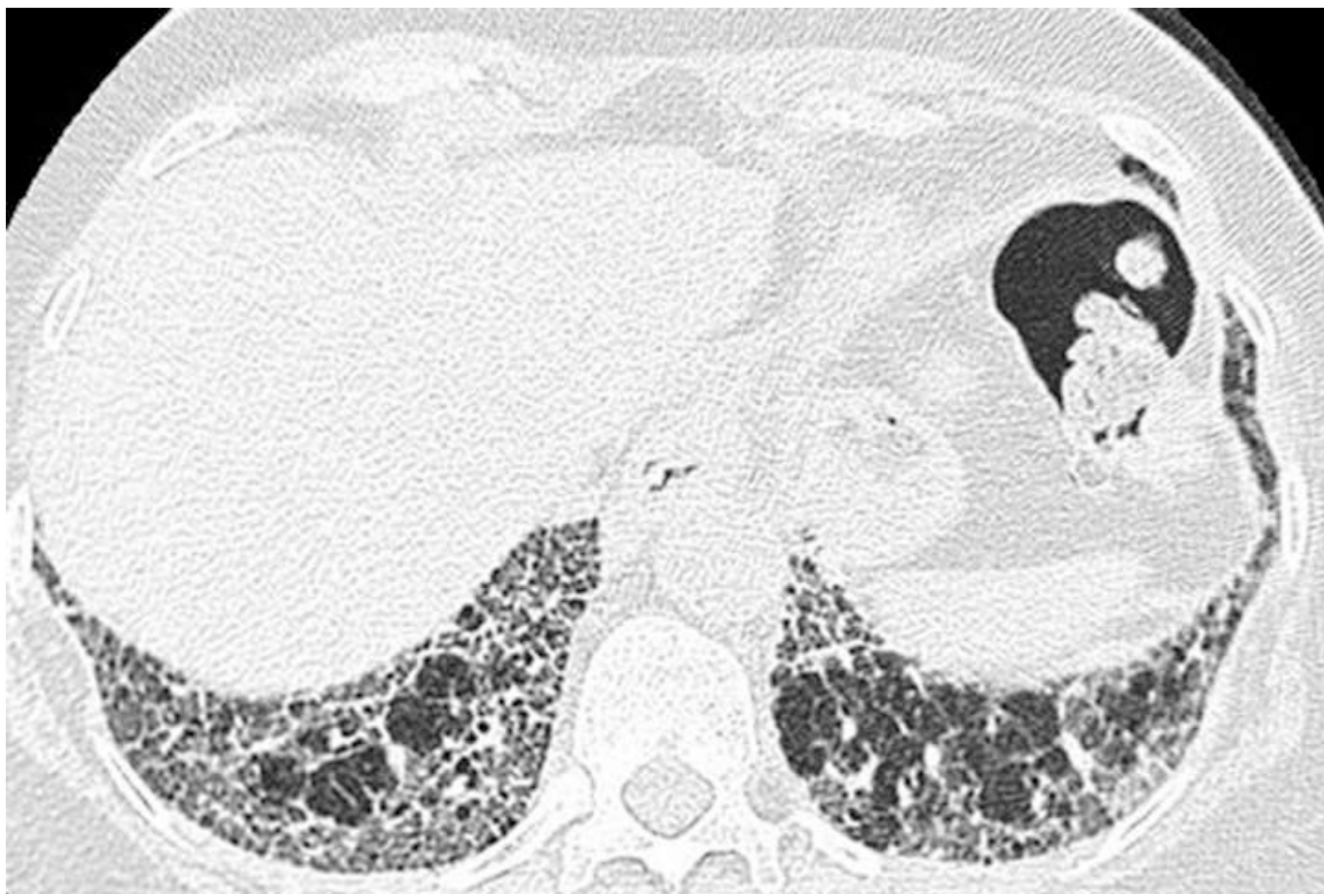
Coronal CT images of a patient with lymphangitic spread of colon cancer demonstrate the thickening of both interlobular septum (arrowheads) and bronchovascular bundles (arrow).



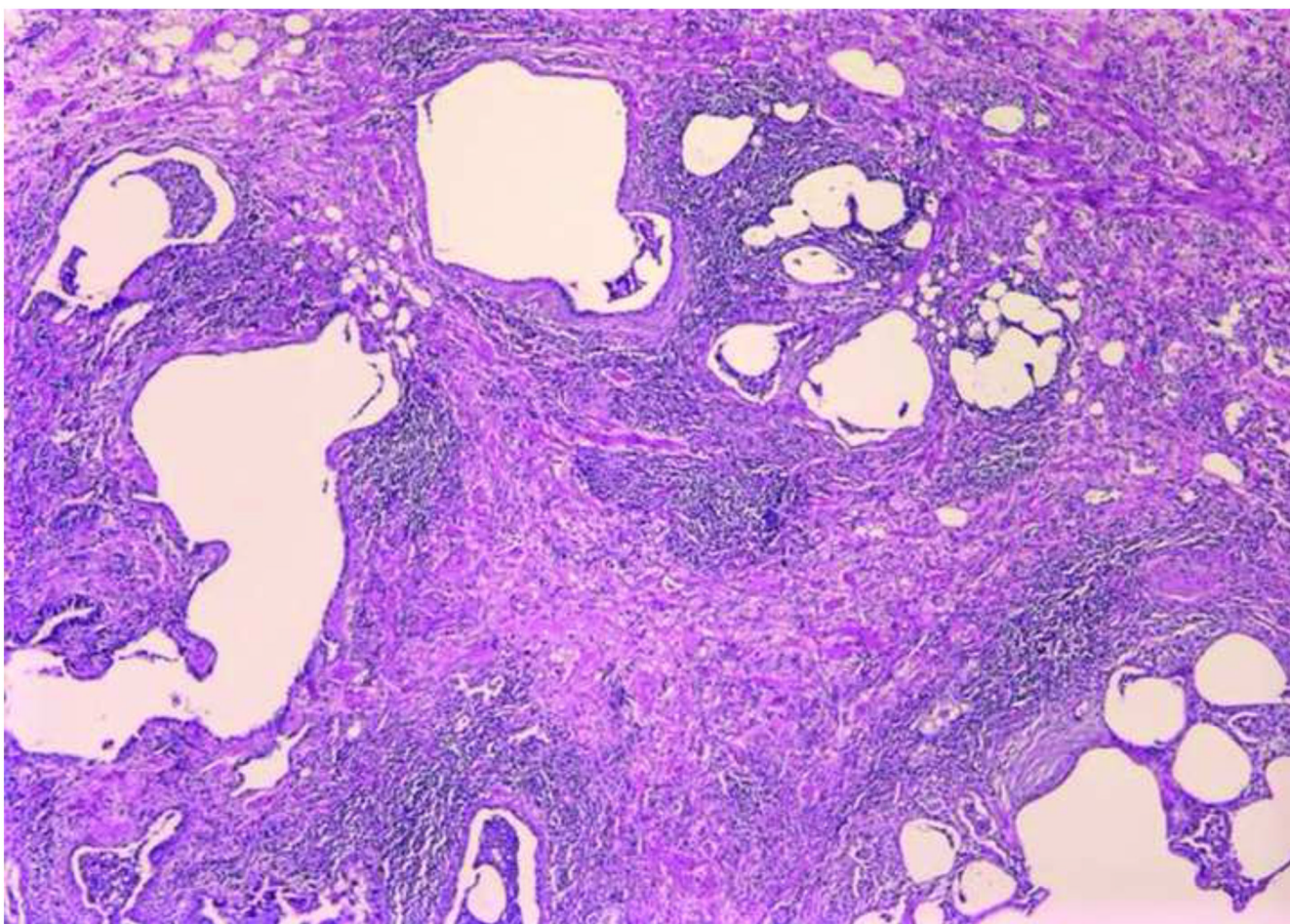
Fig. 5. Centrilobular distribution: Tuberculosis

High-resolution CT image of a patient with tuberculosis demonstrates ill-defined nodular opacities along the bronchovascular bundles, sparing the interlobular septum.

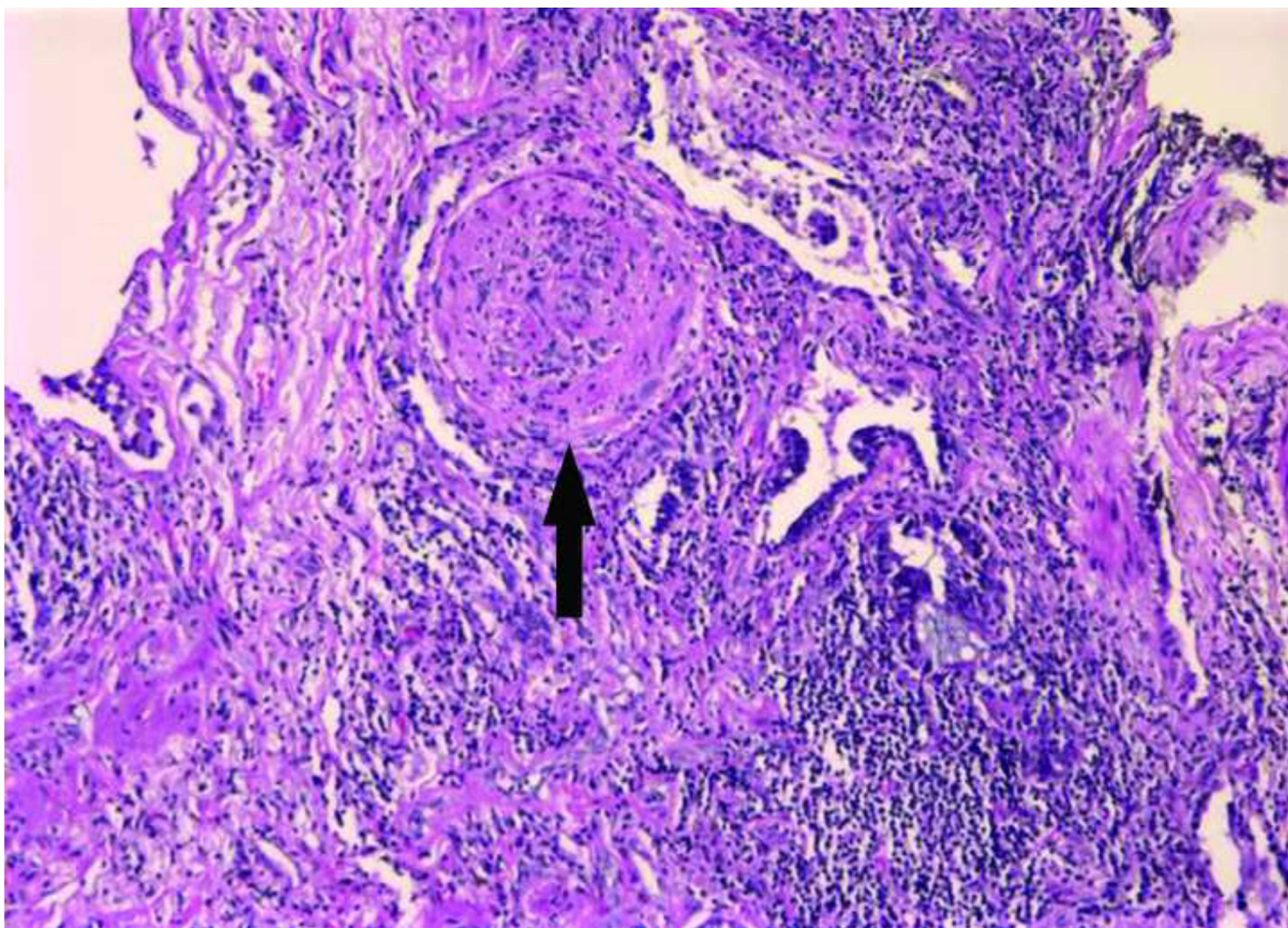
A



B



c

**Figure 6. Idiopathic pulmonary fibrosis**

A. High-resolution CT image shows a diffuse lung disease with peripheral and basilar distribution and honeycombing, indicating IPF/Collagen vascular disease/asbestosis.

B, C. Photomicrograph (original magnification, B: $\times 10$, C: $\times 40$; hematoxylin-eosin stain) of the biopsy specimen showed interstitial fibrosis with honeycombing, with the fibroblastic foci (arrow, C) suggesting end-stage fibrosis.

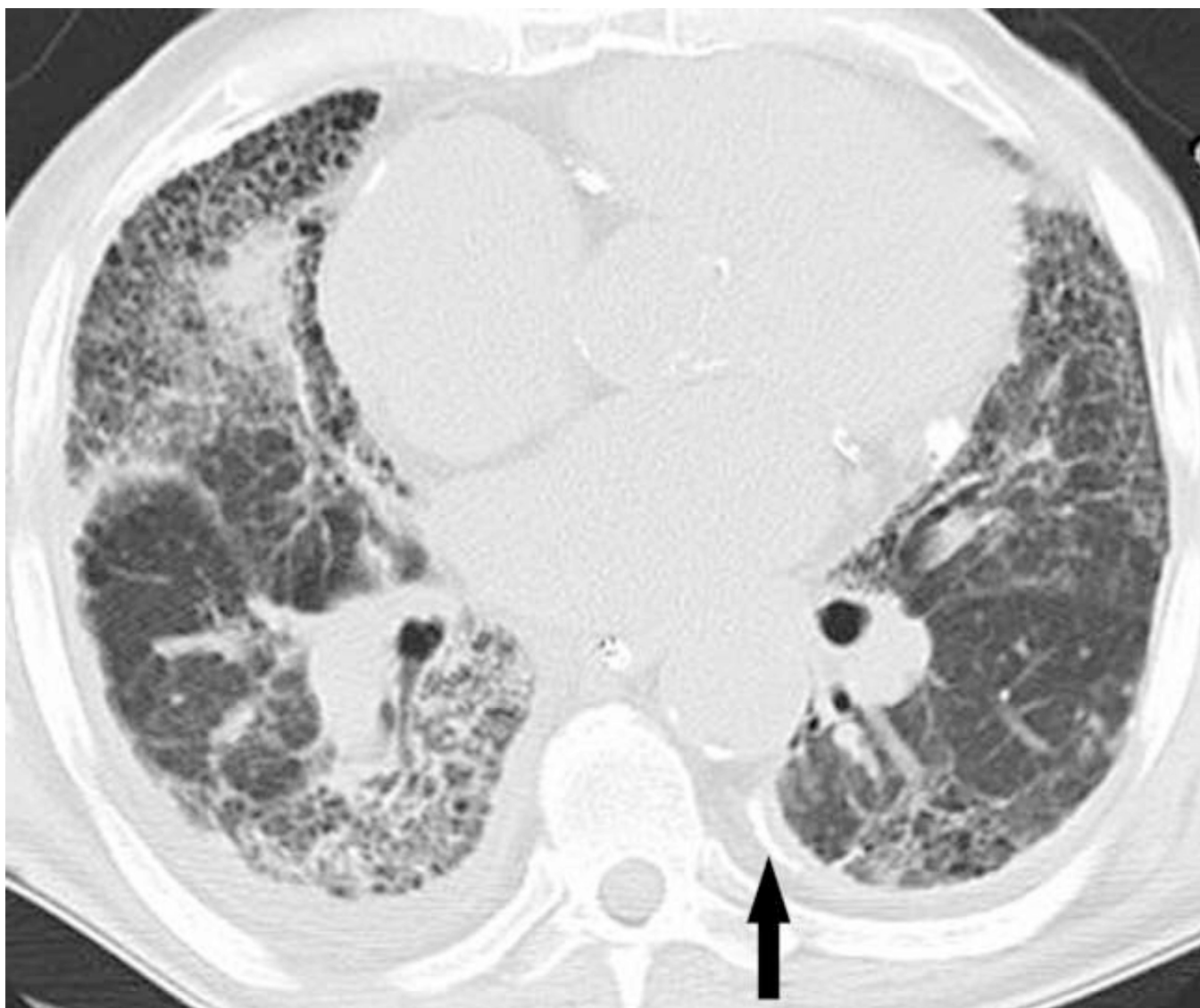
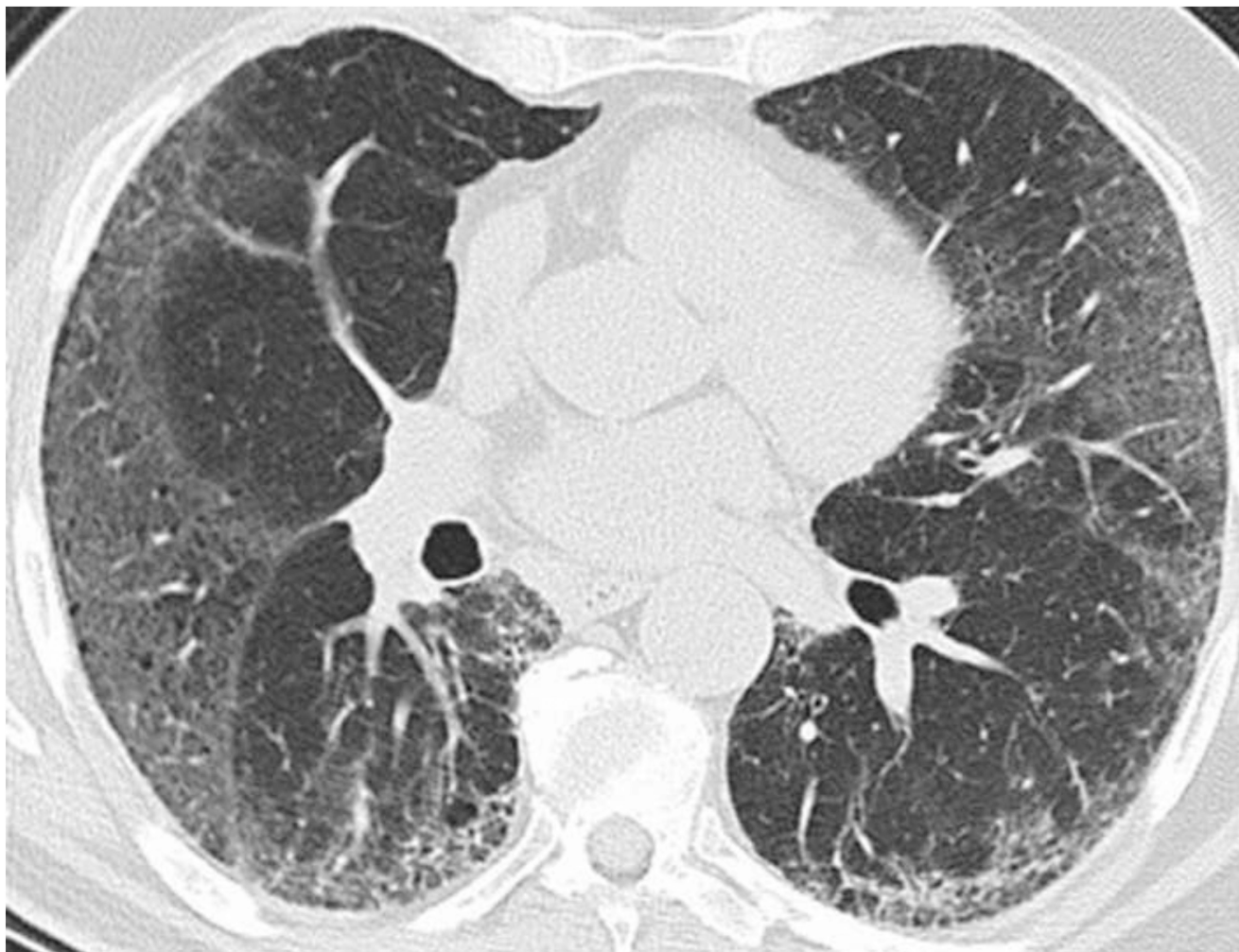


Figure 7. Asbestosis

High-resolution CT image of the lung shows a diffuse lung disease with peripheral and basilar distribution, demonstrating honeycombing. Pleural thickening and calcified pleural plaques are noted (arrow), indicating asbestosis.

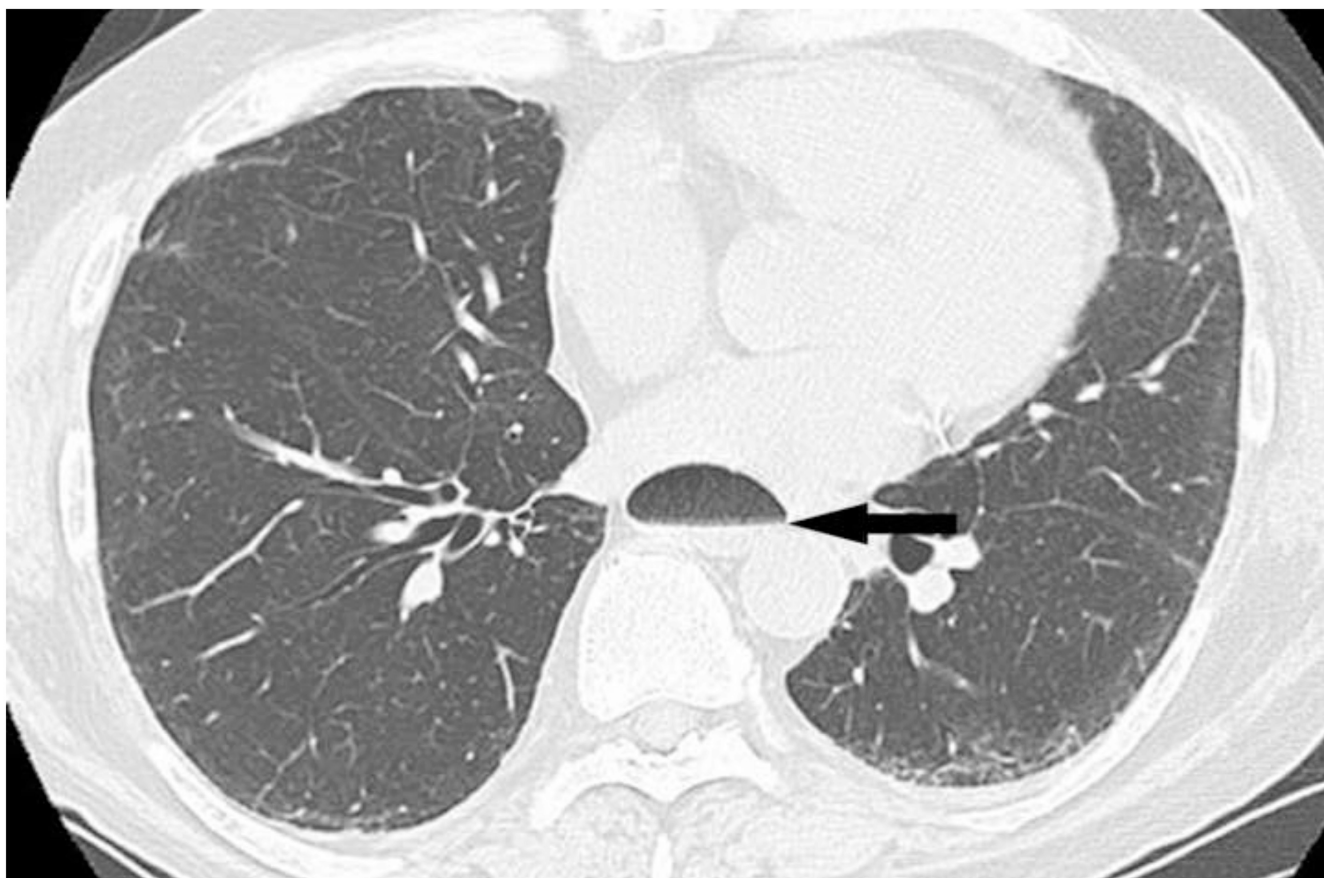
A

B

**Figure 8. Non-specific interstitial pneumonia**

A, B. High-resolution CT images of a patient with NSIP shows a diffuse lung disease with peripheral distribution, demonstrating ground glass opacities, traction bronchiectasis/bronchiolectasis, without definite honeycombing.

A



B

**Figure 9. Scleroderma**

A, B. High-resolution CT images show a diffuse lung disease with peripheral and basilar distribution, demonstrating interlobular septal thickening, ground glass opacities and traction bronchiolectasis, without definite honeycombing, representing NSIP pattern. Note the dilated esophagus with an air-fluid level (arrow, A), suggesting collagen vascular disease, in this case, scleroderma.

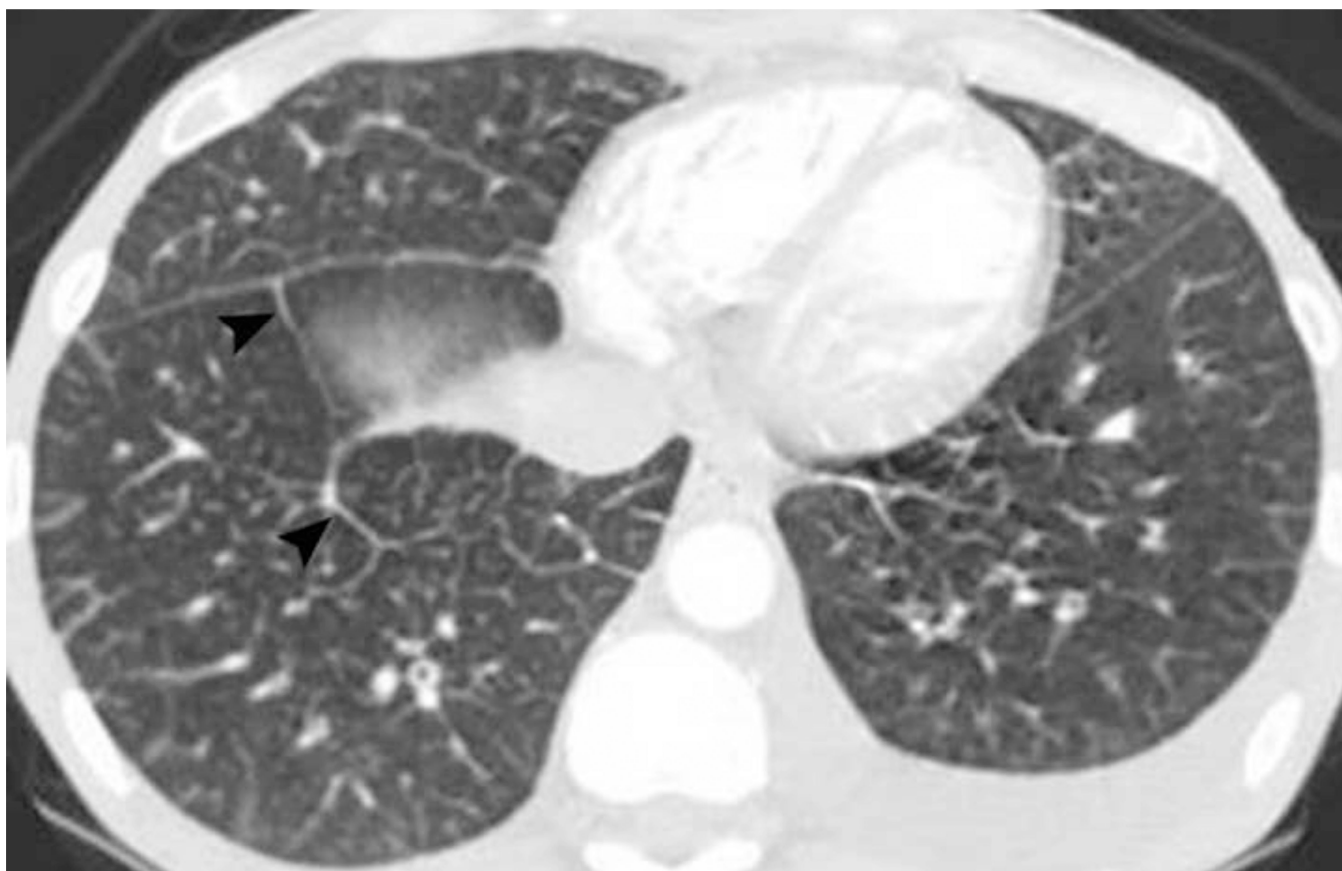


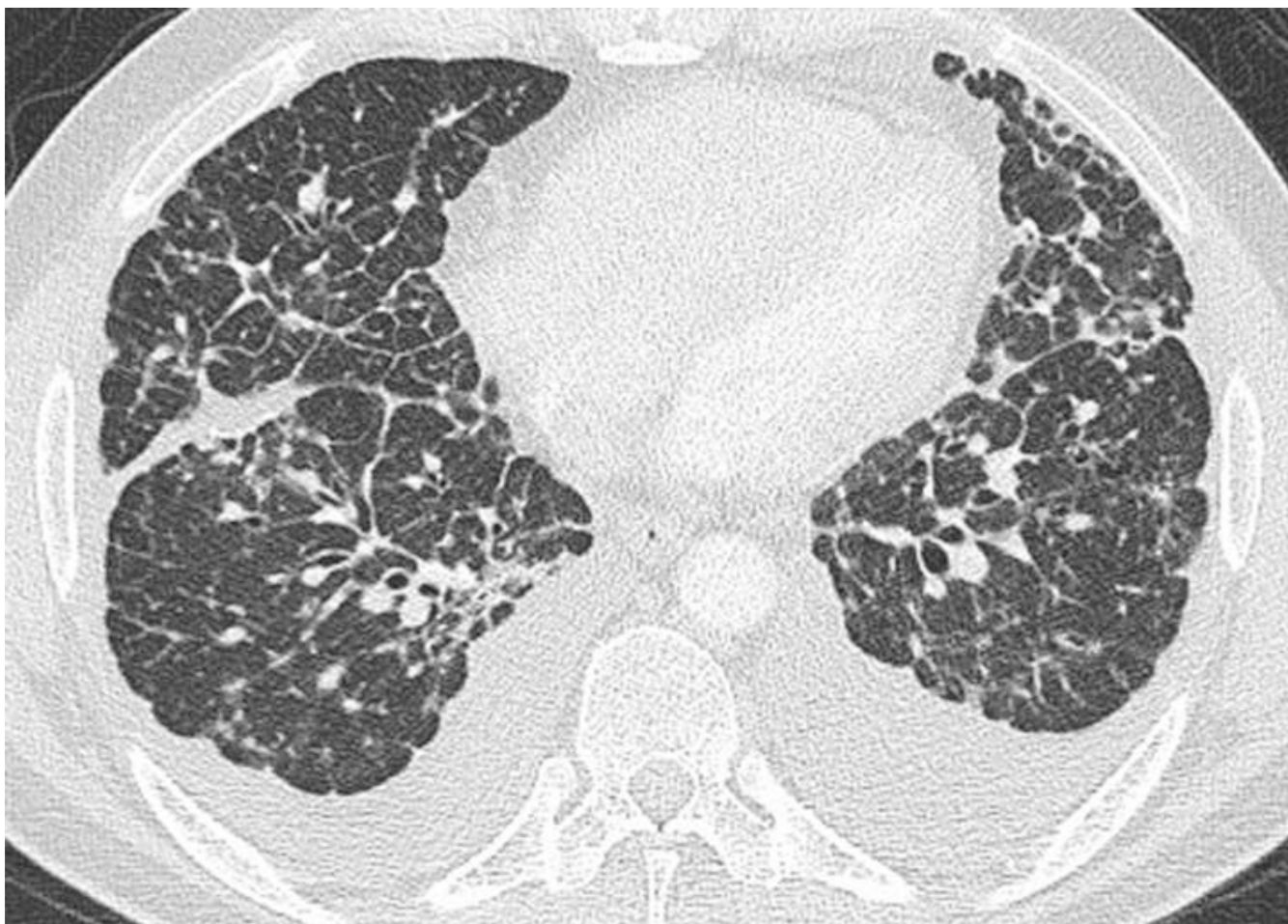
Figure 10. Pulmonary edema

CT scan of a patient with dyspnea on exertion demonstrate smooth interlobular septal thickening at the lung bases (arrowheads), associated with left pleural effusion, representing pulmonary edema.



Figure 11. Sarcoidosis

High-resolution CT image demonstrates a nodular thickening of bronchovascular bundles, interlobular septum and fissures, representing characteristic findings in pulmonary sarcoidosis.

A

B



Figure 12. Lymphatic pattern: lymphangitic spread of tumor

A, B. High-resolution CT images of the lower lungs demonstrate irregular thickening of the interlobular septum and bronchovascular bundles, representing a “lymphatic pattern” due to lymphangitic spread of tumor.

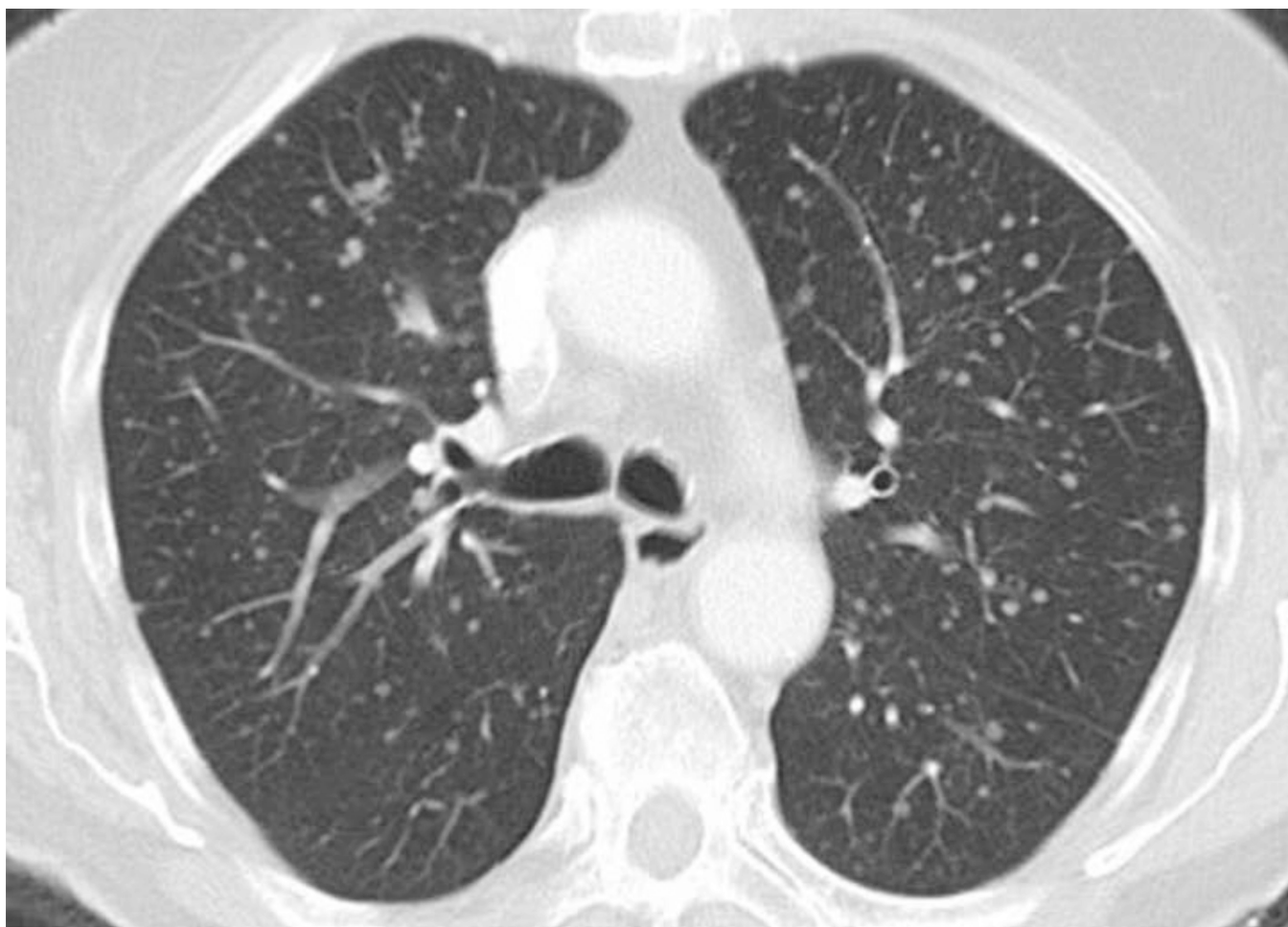


Figure 13. Fine nodules: metastasis

High-resolution CT image demonstrates multiple fine discrete nodules in random distribution, representing miliary metastasis from thyroid cancer.

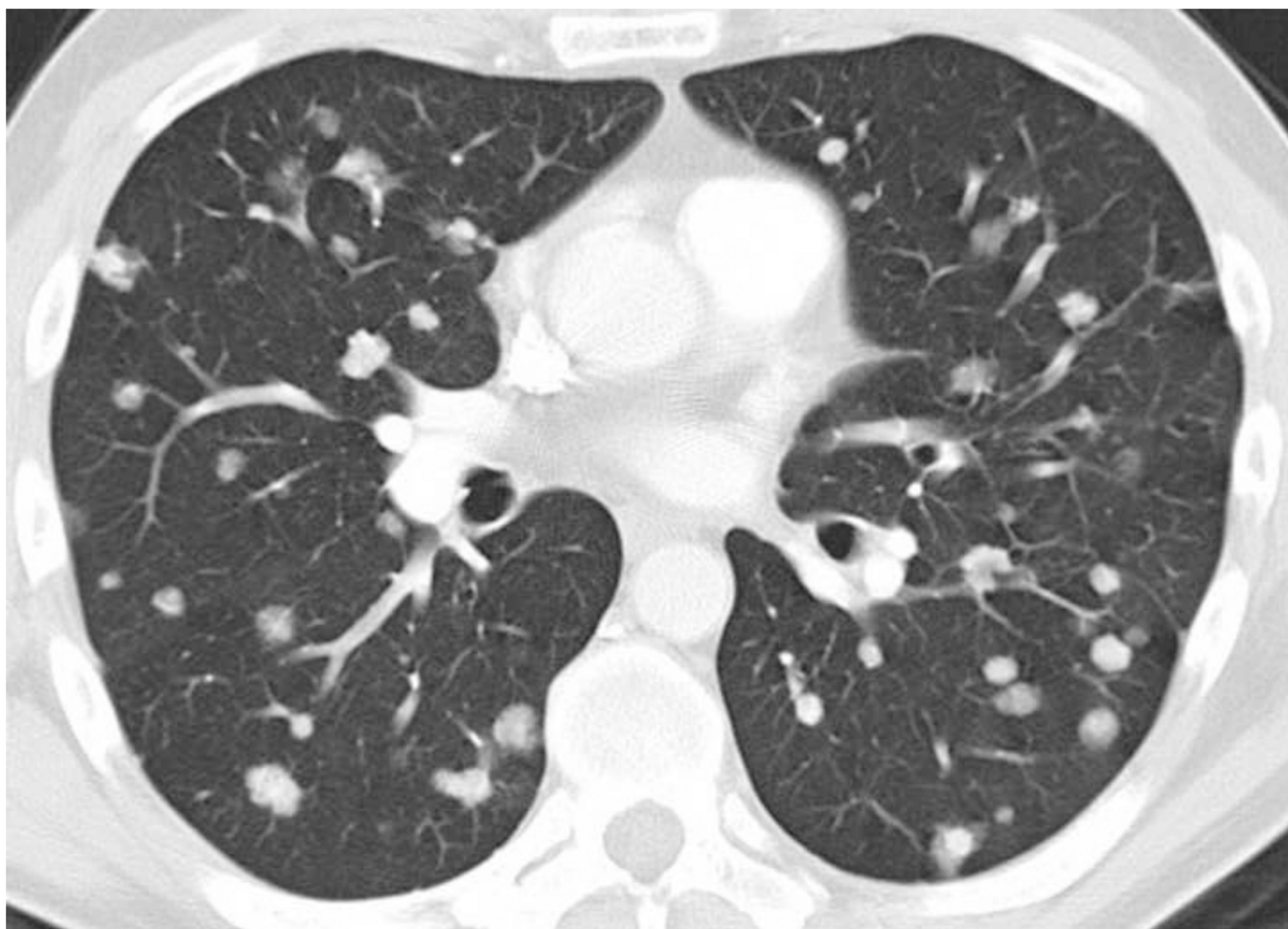


Figure 14. Medium to large nodules: metastasis

High-resolution CT image demonstrates multiple nodules varying in size, mostly medium to large, representing metastasis from lung cancer.



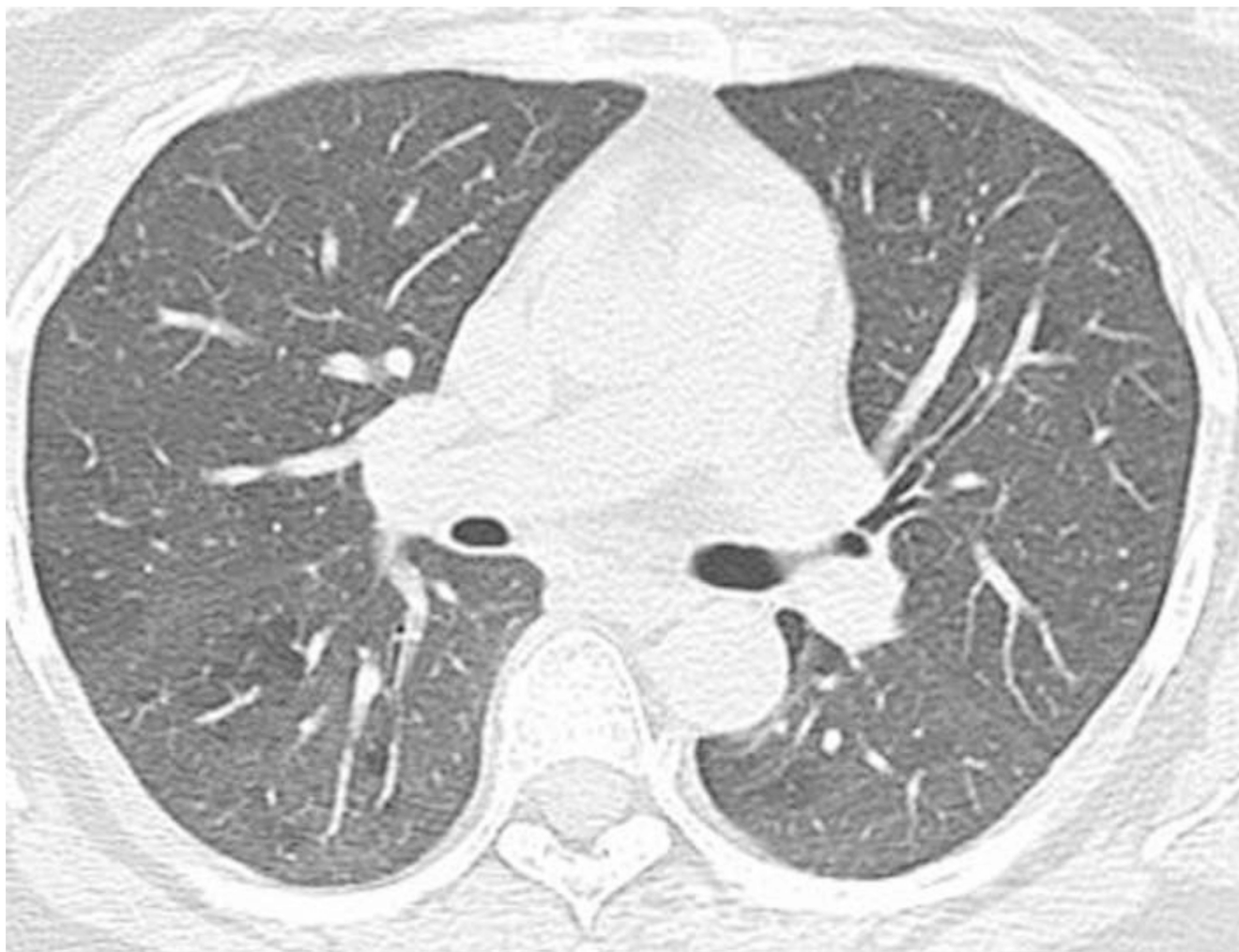
Figure 15. Mycoplasma pneumonia

High-resolution CT image of a 29-year-old female patient with fever shows ill-defined centrilobular nodules, suggesting infectious etiology.



Figure 16. Mycobacterium avium-intracellulare infection

High-resolution CT image of a 69-year-old male with productive cough and hemoptysis demonstrates multiple branching opacities due to impacted impacted centrilobular bronchioles representing “tree-in-bud” appearance, associated with diffuse bronchiectasis.

A

B



Figure 17. Hypersensitivity pneumonitis

A. High-resolution CT image at end-inspiration demonstrates diffuse ground glass opacities.

B. High-resolution CT image at end-expiration demonstrates areas of air trapping as more radiolucent areas, compared to the surrounding lung (arrows).



Figure 18. *Pneumocystis carinii* pneumonia

High-resolution CT image of an HIV positive patient with fever demonstrates diffuse ground glass opacities in bilateral lungs.

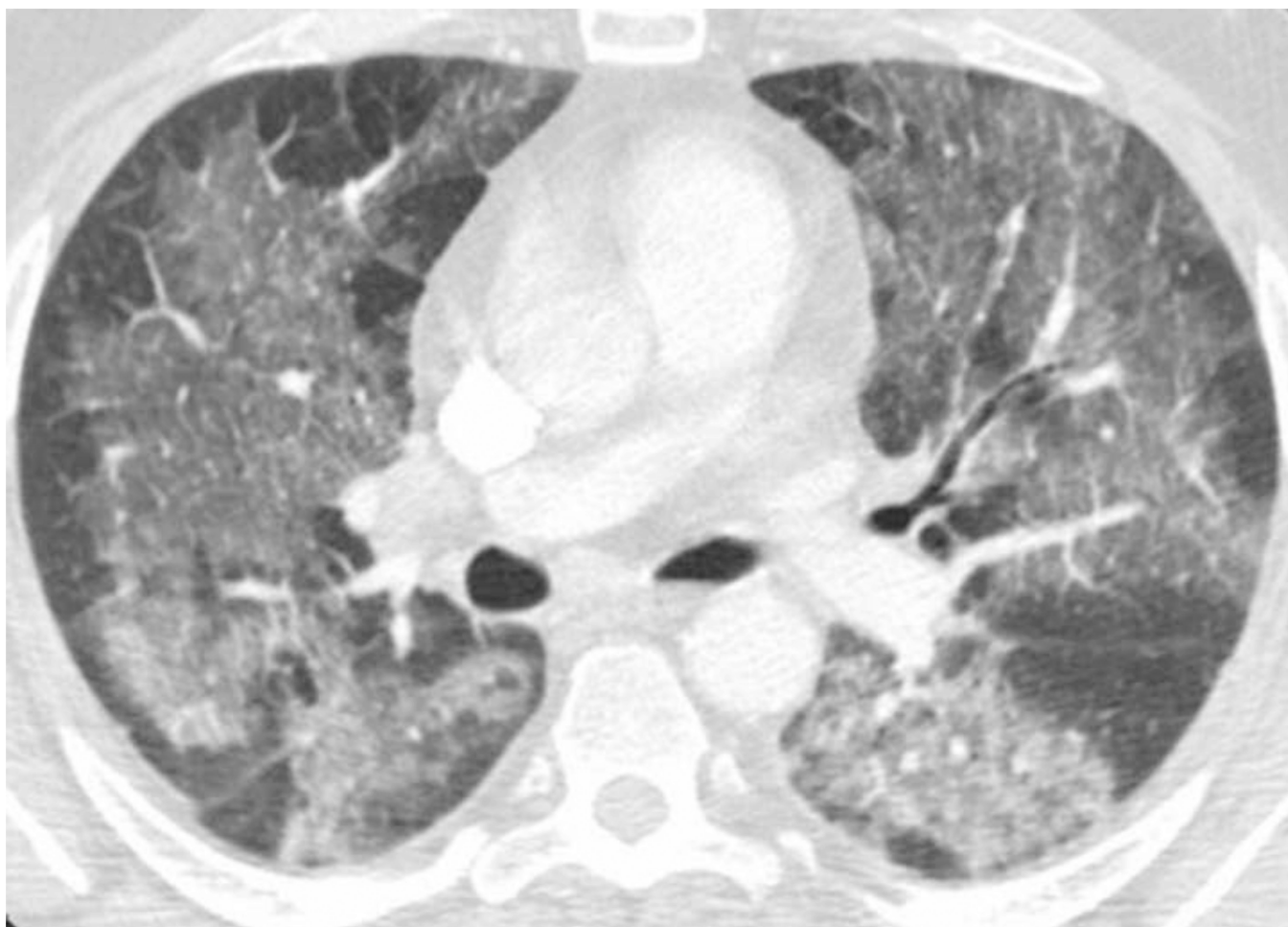
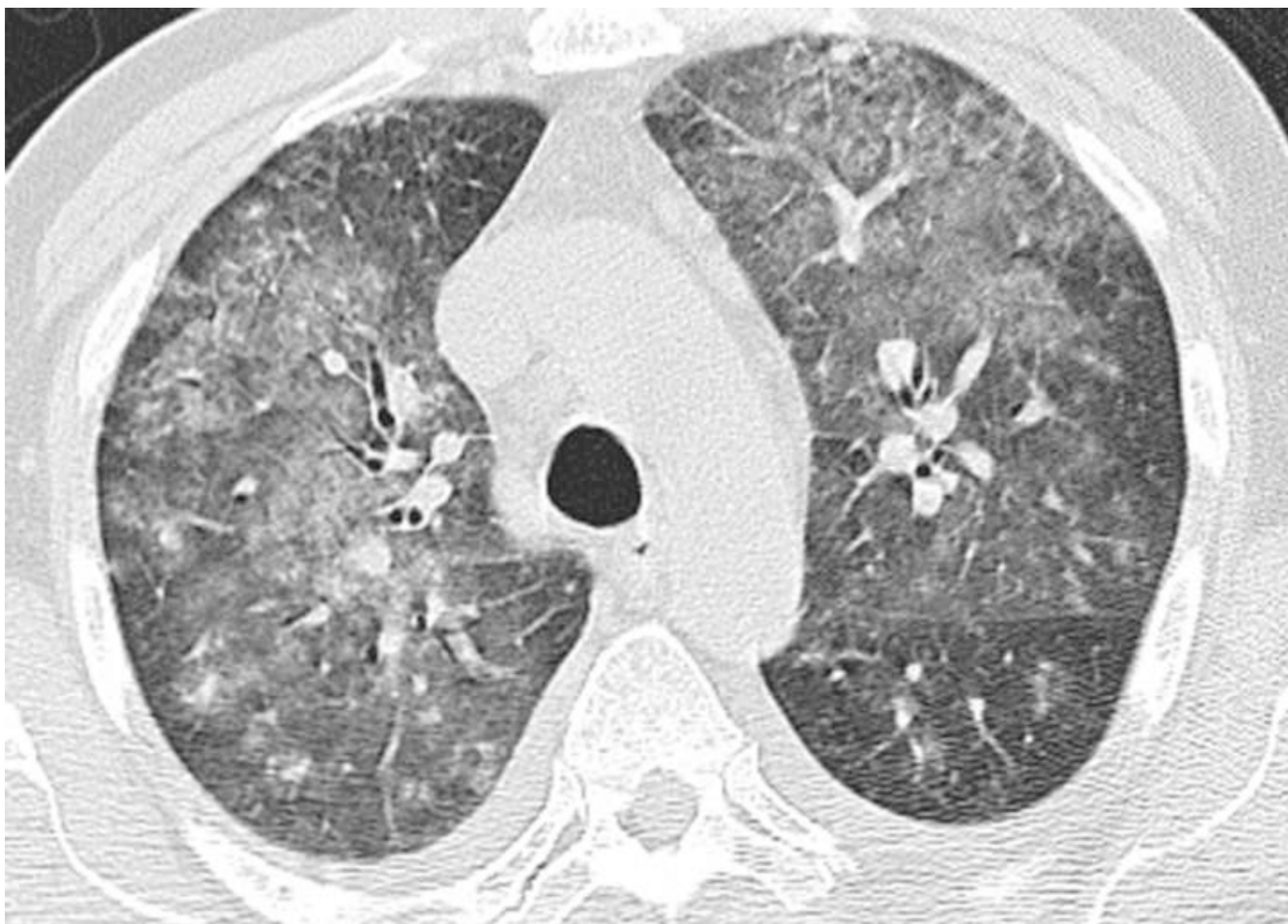


Figure 19. Pulmonary edema

High-resolution CT image in a patient with congestive heart failure shows diffuse groundglass opacities with somewhat central distribution, sparing the subpleural area.

A

B

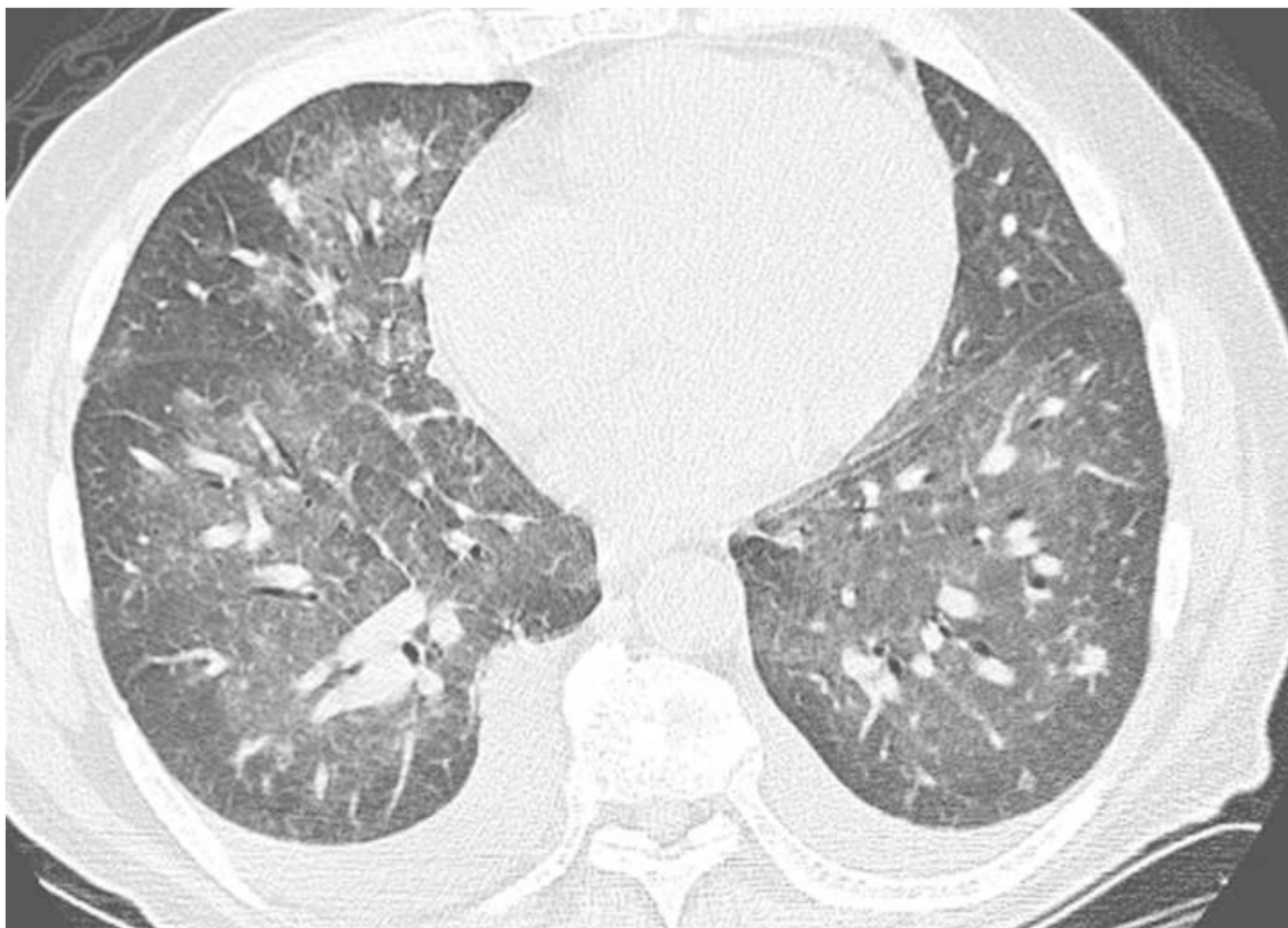
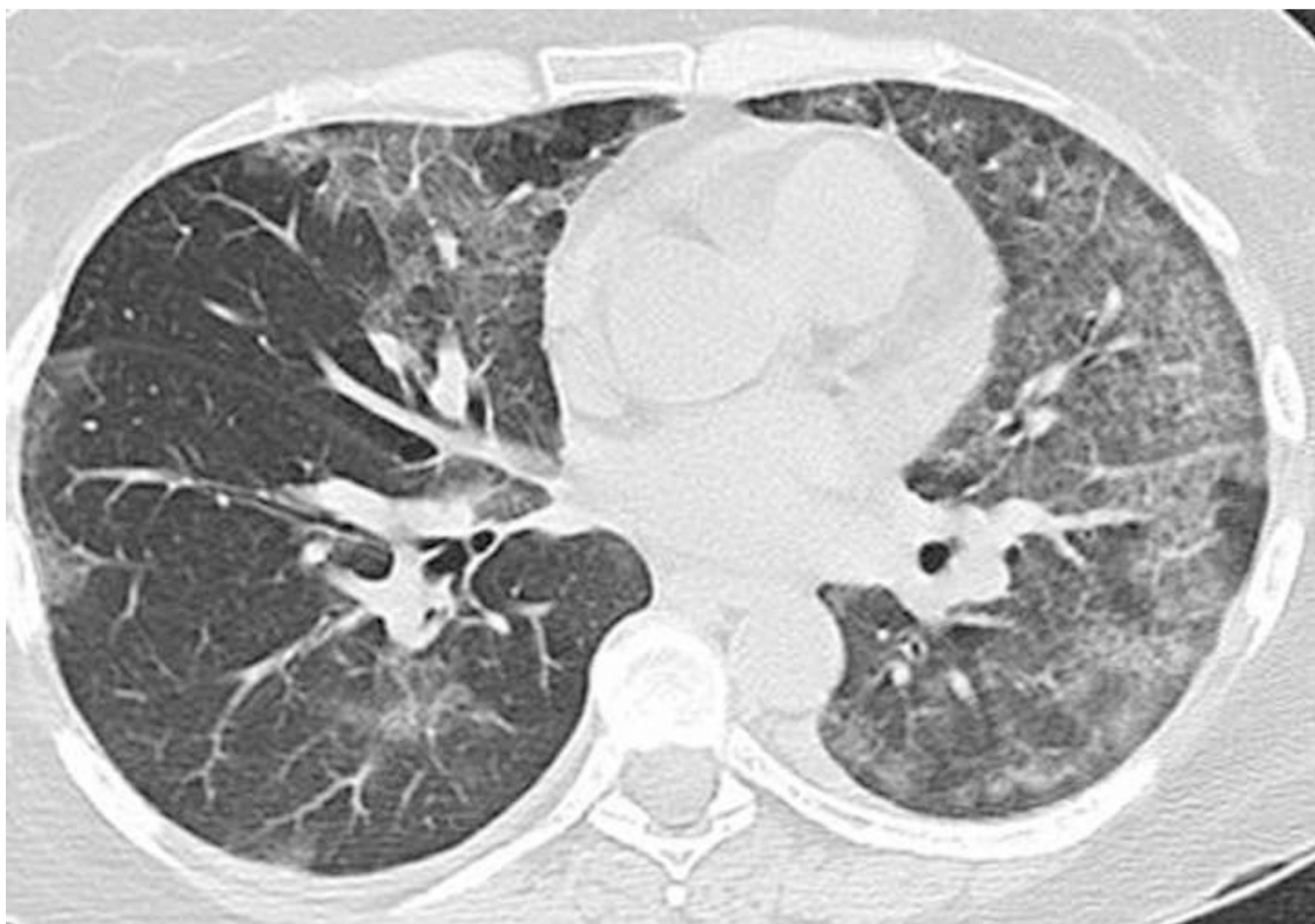


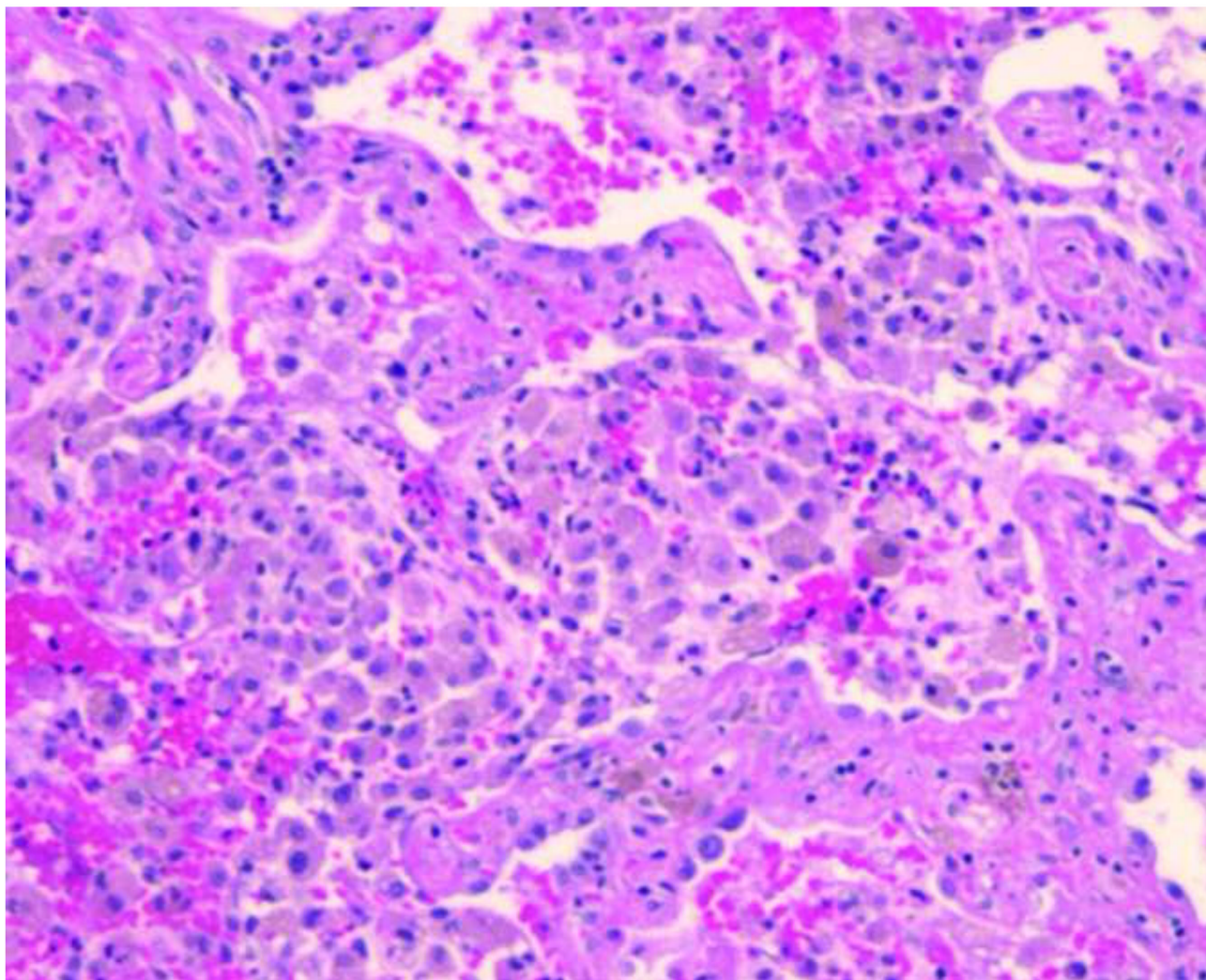
Figure 20. Diffuse pulmonary hemorrhage

A, B. High-resolution CT images in a 58-year-old man with hemoptysis demonstrate diffuse ground glass opacities throughout the lungs representing diffuse pulmonary hemorrhage, with bilateral pleural effusion.

A

B

c

**Figure 21. Desquamative interstitial pneumonia**

A, B. High-resolution CT images of a 49-year-old woman with history of heavy smoking show ground glass opacities with patchy and somewhat peripheral distribution, as well as mild septal thickening.

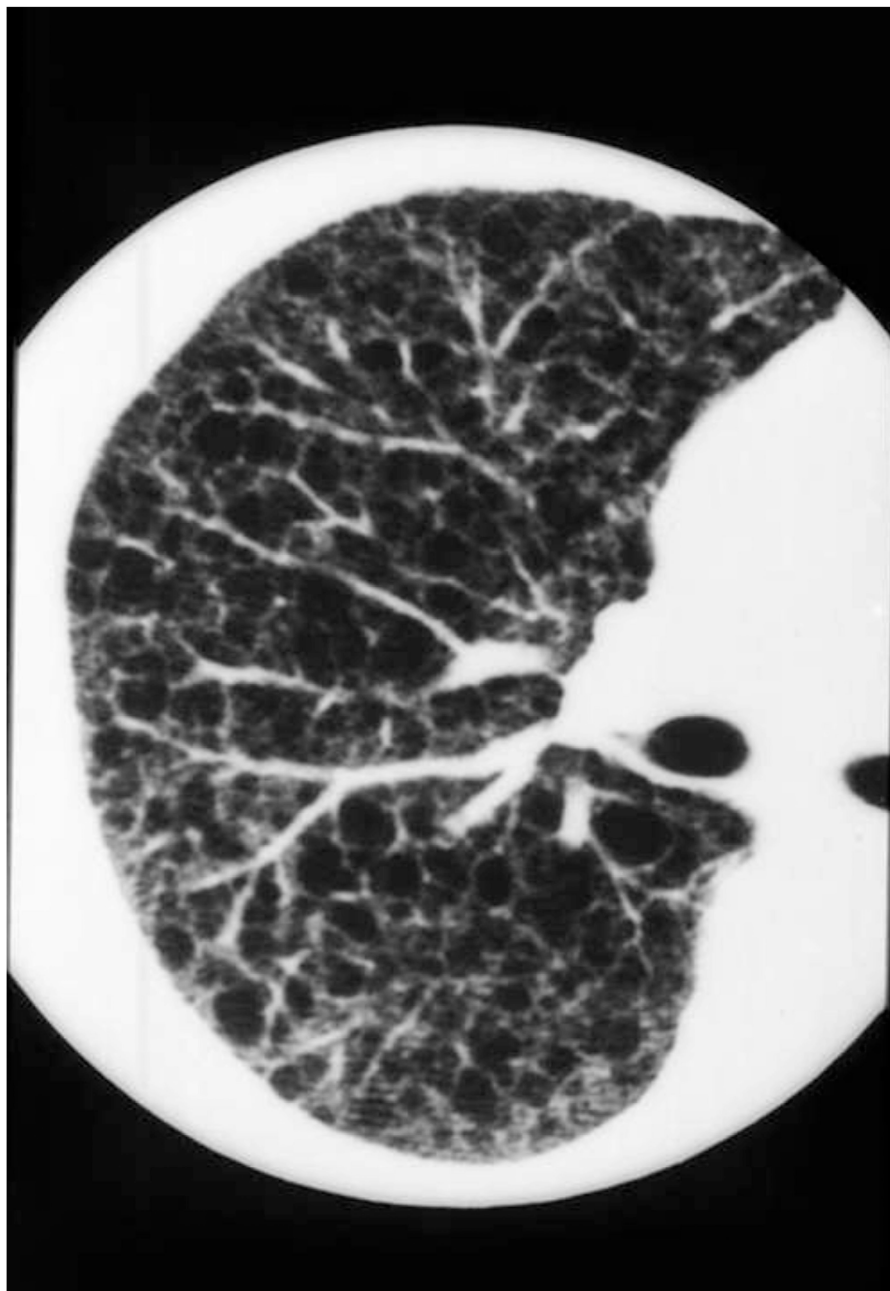
C. Photomicrograph (original magnification, $\times 40$, hematoxylin-eosin stain) shows accumulation of macrophages in alveolar spaces.



Figure 22. Pulmonary Langerhans cell histiocytosis

High-resolution CT image of a 28-year-old woman with history of smoking shows cysts with nodular-appearing walls as well as small cavitary nodules, predominantly in upper lung distribution.

A



B

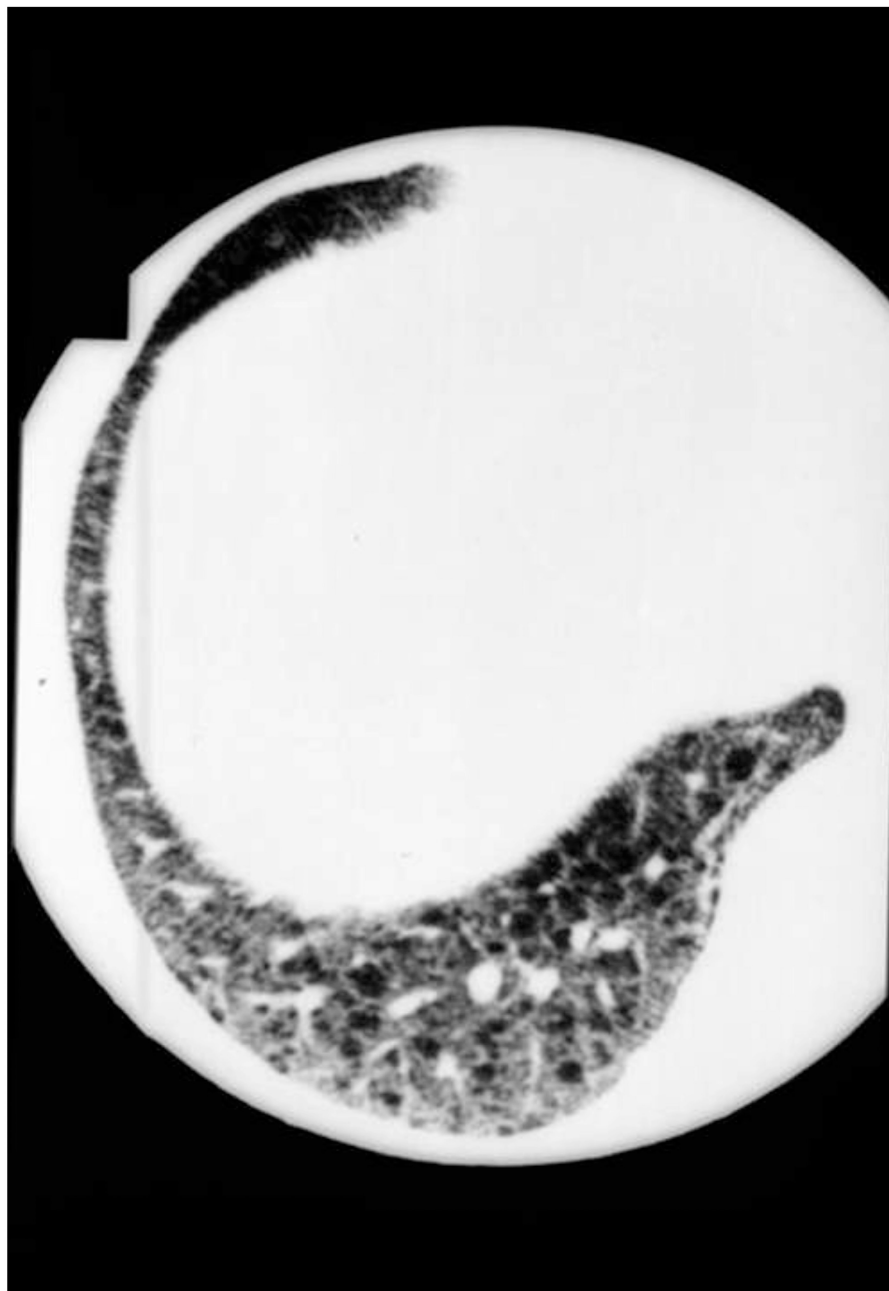


Figure 23. Lymphangioleiomyomatosis

A, B. High-resolution CT images of a young female patient with LAM demonstrates multiple thin-walled cystic changes associated with ground glass opacities throughout the lung, including the costophrenic angle.



Figure 24. Invasive aspergillosis

High-resolution CT image of a 54-year-old man with myelodysplastic syndrome, neutropenia and fever, demonstrates multiple ill-defined nodular opacities surrounded by ground glass opacities, and consolidations with air-bronchogram.



Figure 25. Bronchioalveolar cell carcinoma

High-resolution CT image of a patient with bronchioalveolar cell carcinoma demonstrate multiple parenchymal opacities in both lungs. Differentiation between other neoplastic or infectious processes is difficult based on imaging findings alone.



Figure 26. Cryptogenic organizing pneumonia

High-resolution CT image of a patient with recurrent pneumonia shows parenchymal opacities with characteristically peripheral distribution in bilateral lungs.

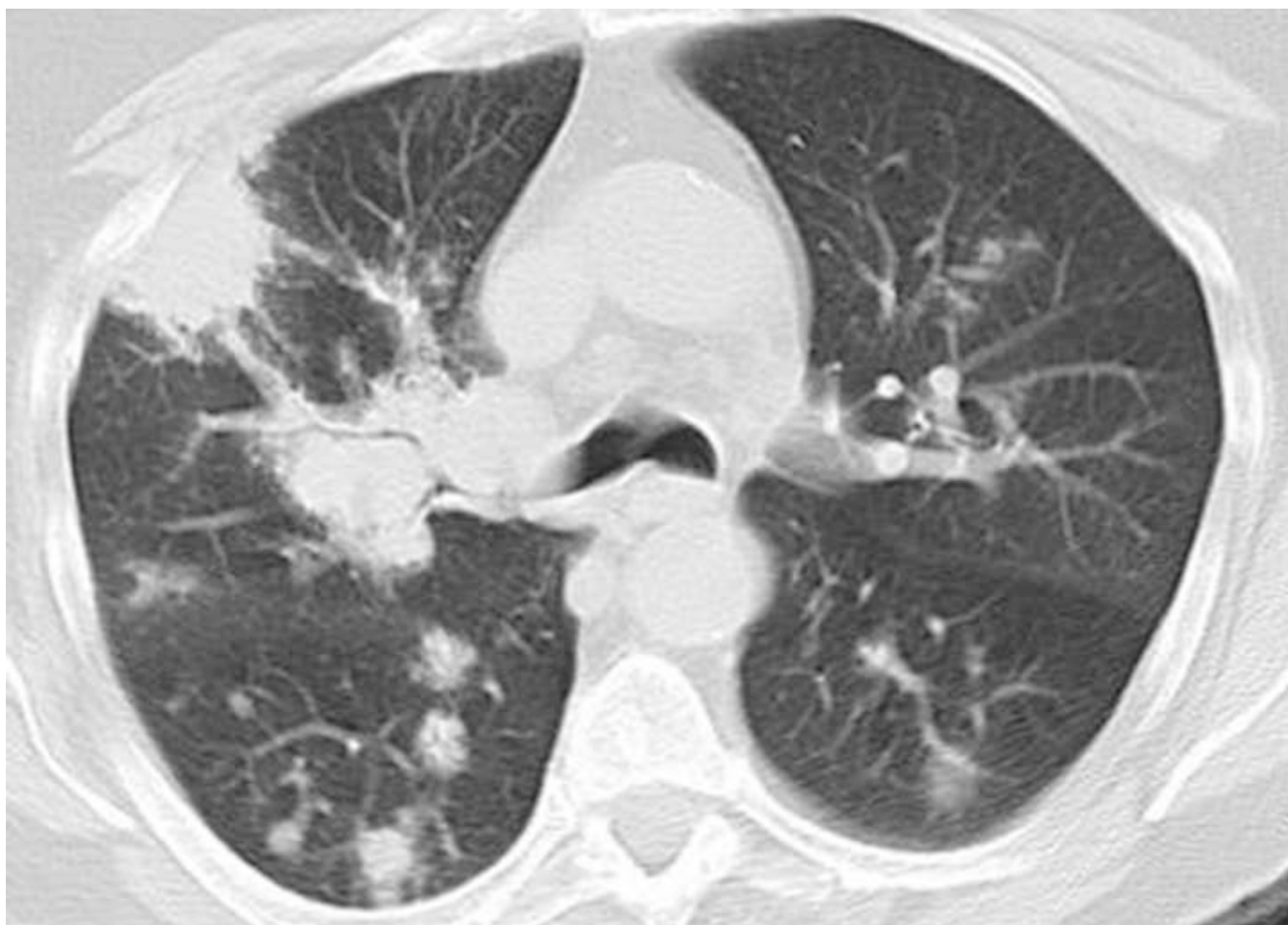


Figure 27. Wegener's granulomatosis

High-resolution CT image of a 69-year-old woman with cough and sinusitis demonstrates multiple ill-defined opacities varying in size and appearance.

**Figure 28. Septic emboli**

High-resolution CT image of a 36-year-old woman with chronic renal failure and abscess demonstrates multiple ill-defined opacities in peripheral distribution associated with pleural effusion.

Table 1

Useful “patterns” in relation to distributions and major differential diagnosis

Diseases of the lymphatic system	
<ul style="list-style-type: none"> • Pulmonary edema • Sarcoidosis • Lymphangitic spread of tumor • Lymphoma 	
Nodular lung disease	
1. Random nodules	
○	<p>“Fine” nodules (approximately 3 mm or less)</p> <ul style="list-style-type: none"> ▪ Miliary tuberculosis ▪ Metastasis ▪ Disseminated fungal infection
○	<p>“Medium or large” sized nodules (> 3mm)</p> <ul style="list-style-type: none"> ▪ Metastasis, metastasis, and metastasis
2. Centrilobular nodules	
○	Variety of diseases affecting centrilobular bronchioles
○	Usually benign and due to infection or inflammation, except for neoplasm spreading along the airway such as bronchoalveolar carcinoma or lymphoma
3. Nodules in lymphatic distribution	
○	Sarcoidosis
○	(could also be lymphangitic spread of tumor or lymphoma)

Table 2

Advanced problems in the interpretation of diffuse lung disease

Smoking-related diffuse lung diseases	
<ul style="list-style-type: none"> • Respiratory bronchiolitis-associated interstitial lung Disease (RB-ILD) • Desquamative interstitial pneumonia (DIP) • Langerhans cell histiocytosis (LCH) 	
Diffuse lung disease with increased lung volumes	
<ul style="list-style-type: none"> • Lymphangioleiomyomatosis (LAM) • Langerhans cell histiocytosis (LCH) • Emphysema with fibrosis 	
Bilateral multiple parenchymal opacities	
<ul style="list-style-type: none"> • Infection • Neoplasm • Cryptogenic Organizing Pneumonia • Chronic Eosinophilic Pneumonia • Vasculitis <ul style="list-style-type: none"> ○ Wegener's granulomatosis ○ Allergic angiitis and granulomatosis (Churg-Strauss syndrome) • Thromboembolic diseases <ul style="list-style-type: none"> Pulmonary embolism with infarction Septic embolism 	